TOWARDS MECHANOCHEMICAL GENERATION OF SINGLET OXYGEN

A THESIS SUBMITTED TO

GRADUATE SCHOOL OF ENGINEERING AND SCIENCE

OF BILKENT UNIVERSITY

IN PARTIAL FULLFILMENT OF THE REQUIREMENTS FOR

THE DEGREE OF

MASTER OF SCIENCE

IN

CHEMISTRY

By

Simay Aydonat

December 2018

TOWARDS MECHANOCHEMICAL GENERATION OF SINGLET OXYGEN

By Simay Aydonat

December 2018

We certify that we have read this thesis and that in our opinion it is fully adequate, in scope and in quality, as a thesis for the degree of Master of Science.

_____

Engin Umut Akkaya (Advisor)

_____

Dönüş Tuncel

_____

Ferdi Karadaş

_____

Canan Ünaleroğlu

_____

Özdemir Doğan

Approved for the Graduate School of Engineering and Science:

_____

Ezhan Karaşan

Director of the Graduate School

ABSTRACT

TOWARDS MECHANOCHEMICAL GENERATION OF SINGLET OXYGEN

Simay AYDONAT

MSc. in Chemistry

Advisor: Engin Umut Akkaya

December 2018

Singlet oxygen is a short-lived reactive species which is involved a number of biochemical processes and implicated as the primary photo-generated cytotoxic agent in photodynamic therapy (PDT) of cancer. Precise chemical control of singlet oxygen generation and or storage is therefore of immense interest. In this particular study, the possibility of mechanochemical release of singlet oxygen in cross-linked polymers carrying anthracene 9,10-endoperoxides was explored. 9,10-Diphenylanthracenes are stable at room temperature but undergo thermal cycloreversion when heated to produce singlet oxygen. Thus, a cross-linked polyacrylate was synthesized, incorporating anthracene-endoperoxide modules with chain extensions at the 9,10-positions. Previously in our lab, thermal lability of the anthracene endoperoxides were shown when attached to gold nanorods. In this work, it was demonstrated that on mechanical agitation in a cryogenic ball mill, fluorescence emission due to anthracene units in the polymer is enhanced, with a concomitant generation of singlet oxygen as proved by detection with a selective probe, SOSG. Also, a cross-linked polyacrylate and a PDMS elastomer incorporating anthracene-endoperoxide modules with chain extensions at the 9,10-positions were synthesized as the polymeric matrix for a better manifestation of mechanochemical process.

Keywords: Photodynamic therapy, singlet oxygen, endoperoxide, mechanochemistry, polymerization.

ÖZET

MEKANOKİMYASAL YÖNTEMLERLE SİNGLET OKSİJEN ÜRETİMİ

Simay AYDONAT

Kimya, Yüksek Lisans

Tez Danışmanı: Engin Umut Akkaya

Aralık 2018

Singlet oksijen, bir dizi biyokimyasal proses içeren ve kanser fotodinamik terapisinde birincil foto-kaynaklı sitotoksik ajan olarak rol oynayan kısa ömürlü bir reaktif türdür. Singlet oksijen üretiminin ve/veya depolamanın hassas kimyasal kontrolü bu nedenle büyük ilgi görmektedir. Bu çalışmada, antrasen 9,10-endoperoksitler taşıyan çapraz bağlı polimerlerde singlet oksijenin mekanokimyasal salınım olasılığı araştırılmıştır. 9,10-Difenylanthrasenler oda sıcaklığında kararlıdır, ancak ısıtıldığında termal siklik evirtim geçirerek singlet oksijen üretir. Bu nedenle, 9,10-pozisyonlarında zincir uzantıları olan antrasen-endoperoksit modülleri içeren çapraz bağlı bir poliakrilat sentezlenmiştir. Daha önce yapılan çalışmalarımızda, antrasen endoperoksitlerin altın nano-çubuklarla bağlandığında oluşan termal kararsızlığı gösterilmiştir. Şimdi, bir kriyojenik bilyalı bir değirmende mekanik çalkalama sonrasında, polimerin içindeki antrasen birimlerine bağlı olarak floresan emisyonunun, seçici bir prob olan SOSG ile saptanan singlet oksijen kombinasyonu ile güçlendirildiğini gösterdik. Bu çalışmamızda, çapraz bağlanmış bir poliakrilat ve 9,10-pozisyonlarında zincir uzantıları olan antrasen-endoperoksit modülleri içeren bir PDMS elastomeri, mekanokimyasal prosesin daha açık bir şekilde kanıtlanmasını amaçlayan polimerik matriks olarak sentezlenmiştir.

Anahtar sözcükler: Fotodinamik terapi, singlet oksijen, endoperoksit, mekanokimya, polimerleşme.

Dedicated to my family

Acknowledgement

First of all, I would like to express my sincere gratitude to my supervisor and mentor Prof. Dr. Engin Umut Akkaya for his greatest support, patience, encouragement and never-ending knowledge of science. It was a great pleasure to work with him and he was one of a kind not only as a scientist and a professor, but also as person. I am thankful to him for the things that I have learnt from him and the awesome time in EUA group that he made it possible.

Next, I would like to thank to my thesis committee, Assoc. Prof. Dönüş Tuncel, Ass. Prof. Ferdi Karadaş, Prof. Dr. Özdemir Doğan and Prof. Dr. Canan Ünaleroğlu for their feedbacks and scientific discussions were held.

I am sincerely indebted to the generous support from Asst. Prof. Bilge Baytekin and thanks to her help, the fruitful comments and discussions she offered, I accomplished my project. I am also thankful to Tutku Bedük for her collaborative work for the thermo gravimetric analysis measurements.

I'm also grateful to our past and present group members who I have encountered as many as I can recall, Dr. Özlem Seven, Dr. Serdal Kaya, Dr. Safacan Kölemen, Deniz Yıldız, Abdurrahman Türksoy, Seylan Ayan, Cansu Kaya, Dr. Nisa Yeşilgül, Esma Uçar, Merve Canyurt, Bilge Banu Yağcı, Yeşim

Şahin, Hazal Sena Bedük, Özge Pehlivan, Beste Gündüz and the rest of the EUA members for the great working ambiance in the laboratory. I owe my gratitude to all these members for their helpful attitude and fruitful scientific discussions.

I specifically want to express my sincere thanks to Deniz Yıldız, Abdurrahman Türksoy and Pınar Erdil for making countless hours of work in the laboratory enjoyable and unforgettable. Those days would be meaningless without the family environment that they have created.

It is a pleasure to thank to Volkan Kahraman, for the continuous joy and his precious companionship in this journey. If he didn't make his support available in different forms, this journey would be exhausting, colorless and tedious.

Finally, I owe my deepest gratitude to my one and only family for their unconditional love, support, understanding and patience. There cannot be enough words to describe their meaning for me. Still, I would like to thank to my mother Sibel AYDONAT for providing continuous support and trust throughout my entire life and my father Murat AYDONAT that I know he still keeps his hands on me even if he is gone. Also, I want to thank sincerely to my brother Berkay AYDONAT for becoming a small version of a father and always giving me the priority to become a better person. I wouldn't be here today and writing this thesis without their help.

List of Abbreviations

PDT: Photodynamic Therapy

PS: Photosensitizer

ROS: Reactive Oxygen Species

ISC: Intersystem Crossing

NMR: Nuclear Magnetic Resonance

TLC: Thin-layer Chromatography

TGA: Thermo Gravimetric Analysis

BODIPY: Boron-dipyrromethane, 4,4-difluoro-4-bora-3a,4a-diaza-s-indacene

MB: Methylene Blue

DPBF: 1,3-Diphenylisobenzofuran

SOSG: Singlet Oxygen Sensor Green

RT: Room Temperature

DMSO: Dimethyl Sulfoxide

DCM: Dichloromethane

EtOAc: Ethyl Acetate

THF: Tetrahydrofuran

EtOH: Ethanol

TBAB: Tetrabutylammonium bromide

Pd (PPh_3)$_4$: Tetrakis (triphenylphosphine) palladium (0)

DCC: N, N-dicyclohexylcarbodiimide

DCU: N, N′-dicyclohexylurea

EDC: 1-Ethyl-3-(3-dimethylaminopropyl) carbodiimide

DMAP: 4- (Dimethylamino) pyridine

AIBN: 2,2′-Azobis(2-methylpropionitrile)

PMA: Poly(methyl acrylate)

PDMS: Poly(dimethylsiloxane)

Hz: Hertz

Contents

List of Figures

List of Schemes

CHAPTER I

Introduction

1.1. Photodynamic Therapy

Photodynamic therapy (PDT) is seen as a promising non-invasive treatment modality for certain malignant (skin, head and neck, gastrointestinal, gynecological cancers), premalignant (actinic keratosis), and nonmalignant (psoriasis, AMD-age related macular degeneration) diseases [1] and it is accepted as an alternative treatment since the beginning of twentieth century [1-4]. PDT has started to take attention by the synthesis and application of hematoporphyrin as a photosensitizer [1]. The use of hematoporphyrin derivatives (HPD) to cure neoplastic tissue was studied by Lipson and Schwartz separately in the 1960's. Thus, they have discovered that HPD is highly phototoxic for tumor cells with high affinity whereas it does not for healthy cells [5]. Interest in HPD continued through the 1970's, and a few years later Dougherty and his coworkers reported that tumor stops to grow when HPD and

red light is present in the cells of mice [6]. The first clinical application of PDT was performed who have bladder cancer in 1976 [7]. Subsequently, early-staged patients with gastric cancer [8], lung carcinoma [9], esophageal cancer [10] were diagnosed and treated by PDT [1]. Afterwards, brain tumors [11-14], head and neck tumors [15,16], breast cancer [17-19], intraocular cancer [20-22], pancreatic cancer [23], gynecological tumors [24,25] were also treated by PDT techniques. The scientists were only partially successful on these studies due to the intrinsic limitations of PDT [1] and the treatment narrowed to only early stage patients [26]. PDT has the potential of being very localized and it is highly selective for treatment of various diseases and it does not lead to severe side effects unlike surgery, chemotherapy or radiotherapy. However, it has limitations such as the tissue penetration of light [27] and oxygen concentration [28] to be considered and thence, one should analyze the elements of PDT to have better insight.

1.2. Keystones of Effective Photodynamic Therapy

Photodynamic therapy necessitates three elements which are light, oxygen and a photosensitizer and it cannot be an appropriate treatment without one of these elements. Therefore, better recovery with PDT requires the delivery of light, the presence of singlet oxygen and a convenient photosensitizer.

1.2.1. Photosensitizer in Photodynamic Therapy

1.2.1.1. Photophysics of Photosensitizers

Photosensitizers are capable of producing singlet oxygen which is the main cytotoxic reagent in PDT and that photosensitizer should be irradiated with proper wavelength of light [29-31]. Thus, ground state photosensitizer (singlet ground state) can transform into higher energy states (singlet excited state) by one photon excitation [29]. The short-lived excited state can undergo relaxation either by fluorescence or internal conversions. When the relaxation of PS to its ground state occurs with the emission of light, it is known as fluorescence [29]. In internal conversions, heat can be generated during relaxation of PS instead of emission of light [29]. However, formation of singlet oxygen cannot be achieved by both of these processes. Pathway known as intersystem crossing leads to transition from singlet excited state of photosensitizer to triplet excited state where the generation of singlet oxygen becomes possible [29,30]. Triplet excited state of PS can return back to singlet excited state which is called delayed fluorescence [32] or relax to the ground state known as phosphorescence which have longer lifetime than fluorescence [29]. However, the formation of singlet oxygen strongly depends on the energy transfer from triplet excited state PS to molecular oxygen which is at triplet ground state [29,30]. The schematic representation of these energy transfers is depicted in the following **Figure 1**.

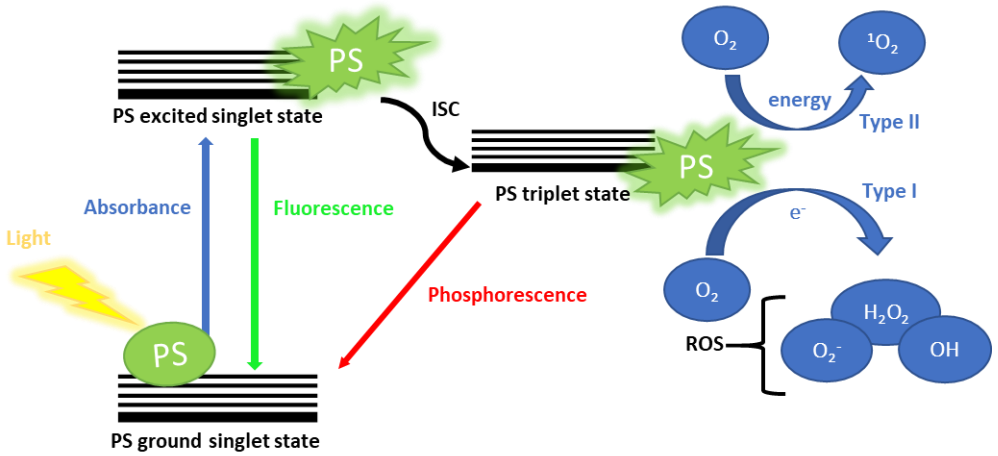

Figure 1: Schematic representation of formation of singlet oxygen on Jablonski Diagram [33].

1.2.1.2. Properties of Ideal Photosensitizer

Selecting the suitable photosensitizer is one of the most crucial steps while forming cytotoxic singlet oxygen in PDT action. An ideal PS should easily be synthesized with good stability and long shelf life [34]. It should show no dark toxicity which means being non-toxic in the absence of light and be easily eliminated from patients. That is, photosensitizers have to be cleared from healthy cells in short time periods to prevent phototoxic side effects. In addition, high triplet quantum yield for ISC and long triplet lifetime are required to give time for generation of singlet oxygen [34]. Red or Near-IR adsorption and high absorption coefficient are counted as other desirable properties [35]. Lastly, targeting moieties on PS improves the efficiency of PDT and so, reduces the possibility of dark toxicity and likely side effects [34].

Photofrin® was the first approved and also the most frequently used photosensitizer in clinical applications throughout the world for different types of cancer [36]. However, PDT with Photofrin® has showed that new sensitizers should be discovered since it has a complicated and uncertain structure, low absorption coefficient, short wavelength (630 nm) and low selectivity. Moreover, it causes skin sensitivity to light [37] and singlet oxygen quantum yield is rather low (0.06-0.12) for PDT applications [38]. Therefore, large concentrations of the Photofrin® and high light intensities are needed for clinical use [39]. Due to these reasons, there has been several attempts to synthesize new photosensitizers that can overcome described issues and list of PS examples can be seen in **Figure 2**.

Trade Name	Indication	λ (nm)	ε (M-1cm-1)	Quantum Yield
Photochlor	Basal-cell carcinoma	665	-	-
Talaporfin	Solid tumors from diverse origins	664	15,800	0.56
Levulan	Basal-cell carcinoma, head and neck, gynecological tumors	635	10,000	0.42
Benzvix	Gastrointentinal cancer	635	10,000	-
Metvix	Basal-cell carcinoma	635	10,000	-
Hexvix	Diagnosis of bladder tumors	400	10,000	-
Photofrin	Cervical, endobronchial, esophageal, bladder, gastric cancers, brain tumors	630	1,170	0.06-0.12
BOPP	Brain tumors	630	-	-
Visudyne	Neovascularization of retina secondary to macular degeneration	689	35,000	0.80
Foscan	Head and neck, prostate, pancreatic tumors	660	30,000	0.58
Pc 4	Cutaneous / subcutaneous lesions	675	84,000	0.38
Purlytin	Cutaneous metastatic breast cancer, basal cell carcinoma, Kaposi's sarcoma, prostate cancer	664	30,347	0.71

Figure 2: List of examples of photosensitizers with their trade names [38].

Foscan®, a chlorine sensitizer was found and the problems related to Photofrin® like need for high concentration of drug/light exposure and long-term photosensitivity was no longer an issue [31]. ALA derivatives such as Levulan®, Metvix®, and Hexvix® are also known by their high potential for treatment as a photosensitizer [31]. Uptake of ALA derivatives is higher in malignant tissues compared to normal tissues by 10 to 1 [40] yet, they have penetration issues (<1cm) and are limited to use, mostly skin cancer [41].

There are also many other sensitizers apart from these described derivatives, which have been used in *in vitro* and *in vivo* studies [42] and some of the commonly used are shown below in **Figure 3** and **Figure 4.**

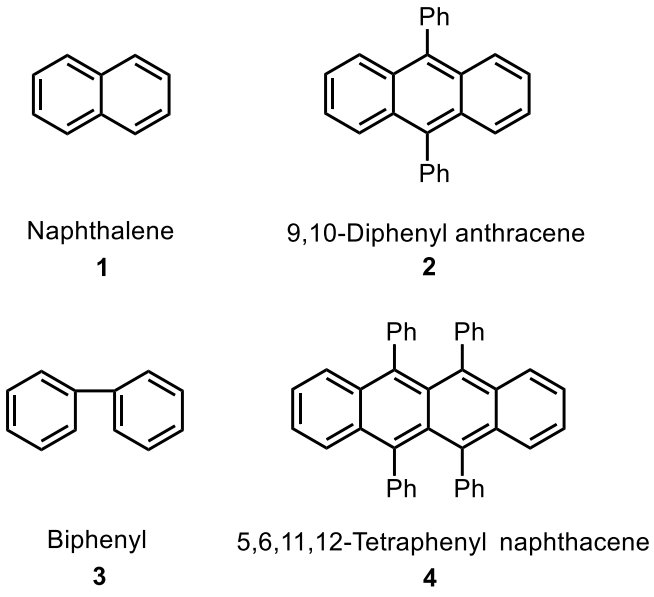

Figure 3: Some examples of chemical structures of common aromatic hydrocarbon singlet oxygen sensitizers.

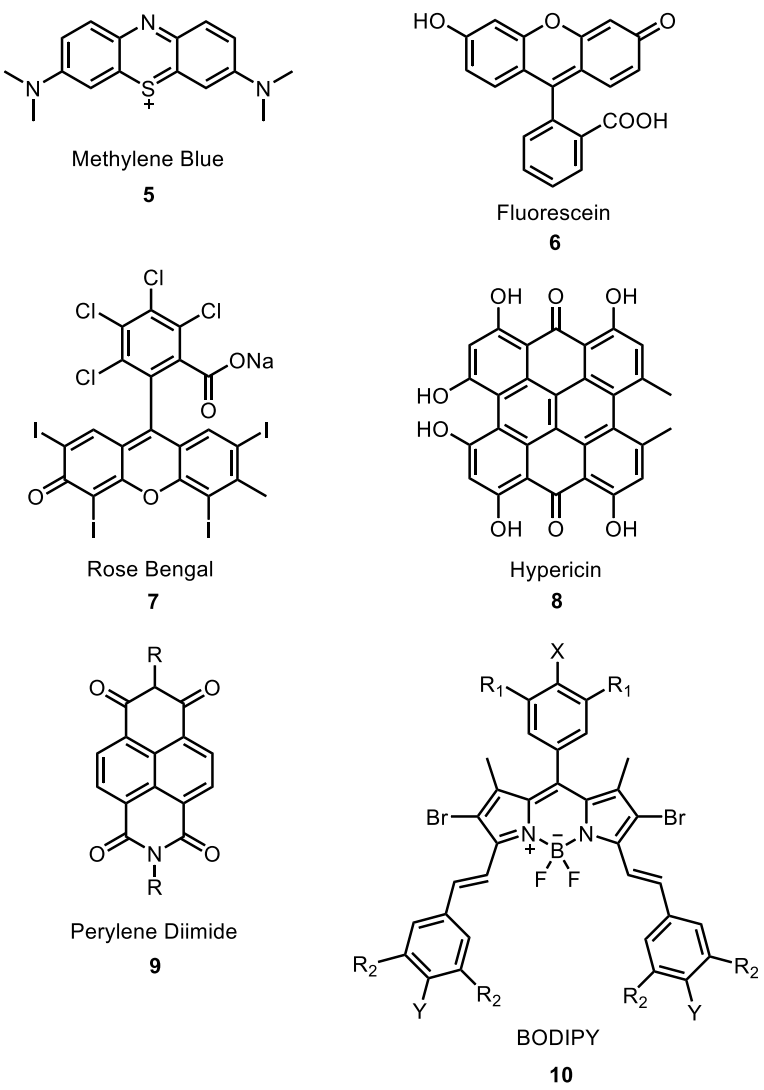

Figure 4: Some examples of chemical structures of common singlet oxygen dve sensitizers.

1.2.2. Light in Photodynamic Therapy

Light source plays a significant role in both the generation of singlet oxygen and the selectivity towards a certain tissue. It is not only crucial for the excitation of photosensitizer but also used to adjust and define the efficiency of PDT [1]. However, it is possible that light which penetrates to tissues can be not delivered and distributed homogenously. In the case of successful delivery of

light to tissues, light can be either absorbed or scattered and delivering light can be struggling in the cell environment due to turbidity [29]. Since turbid medium leads to scattering, penetration of light turns out to be limited.

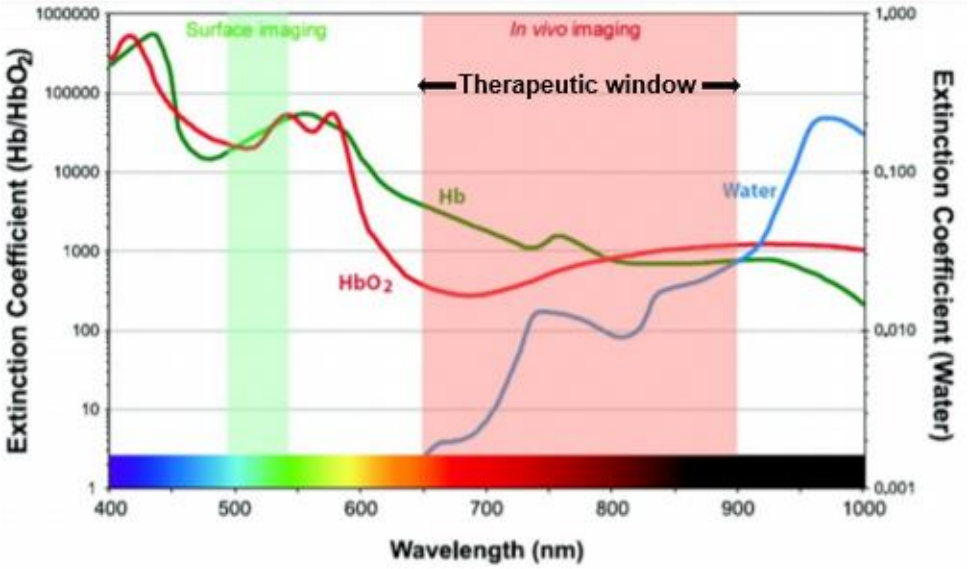

Figure 5: Schematic representation of hemoglobin and water absorbing light depending on wavelength and optical window for PDT. Reprinted with permission from [43]. Copyright © (2010) American Chemical Society.

It is discovered that light in the visible region preferably red and near-IR radiations penetrate to the tissues deeper than the blue light [44]. Most effective range of light lies between 600 and 900 nm known as ‘therapeutic window’ or ‘optical window’ as seen in **Figure 5** [45,46]. The energy of light is not adequate to initiate PDT action and some molecules such as macromolecules, myoglobin, hemoglobin and water [29] absorbs most of the incoming light at longer wavelength than therapeutic window. It should be known that delivery of light,

dose of light, light penetration and light exposure time are very significant for the efficiency on clinical applications.

One should note that choosing the appropriate light source is another need to sustain PDT. Lasers and light emitting diodes (LEDs) are known as most commonly used light sources. Lasers can produce monochromatic light with high intensity and thus, it can irradiate tumors directly and effectively [3, 47]. Secondly, LEDs are found in diverse geometric shapes and sizes and they can be used in various ways such as delivery of light to superficial lesions or tumor implanted delivery of light [3].

1.2.3. Oxygen in Photodynamic Therapy

Tumor destruction occurs in three different ways which are direct killing of tumors, tumor infraction by damaging tumor vasculature and activation of an immune response against cancer cells by the generation of singlet oxygen in the medium [1]. Three pathways controls tumor cells and contributes to the process of cancer killing and these processes are complementary with the oxidant singlet oxygen.

Produced singlet oxygen at target area can react with macromolecules and structural elements of cells and induce cell death [29,48]. Dissolved oxygen is needed to employ such treatment method, however, the absence of oxygen in cancer cells obstruct the treatment [49,50]. Since tumors of most cancer types develop a region of serious hypoxia (absence of molecular oxygen), applying

most therapeutic protocols gets harder. More troublesome, PDT produces acute hypoxia and makes itself a self-limiting method [51]. Therefore, problem of lack of molecular oxygen to be able to generate singlet oxygen in the reaction medium should be solved for better treatment. Detailed information about singlet oxygen will be discussed int the following sections.

1.3. Properties of Singlet Oxygen

1.3.1. Properties & Electronic Structure of Singlet Oxygen

Singlet oxygen ($^1O_2$) is one of the members of reactive species which are called “reactive oxygen species” (ROS) that oxidize biomolecules. Oxygen in its ground state is known necessary for all organisms and biological processes and it is found as molecular oxygen which is also called triplet oxygen in the environment. However, singlet oxygen which is the electronically excited version of molecular oxygen is assumed to take more attention according to the researches and has specific features as in **Figure 6** [52].

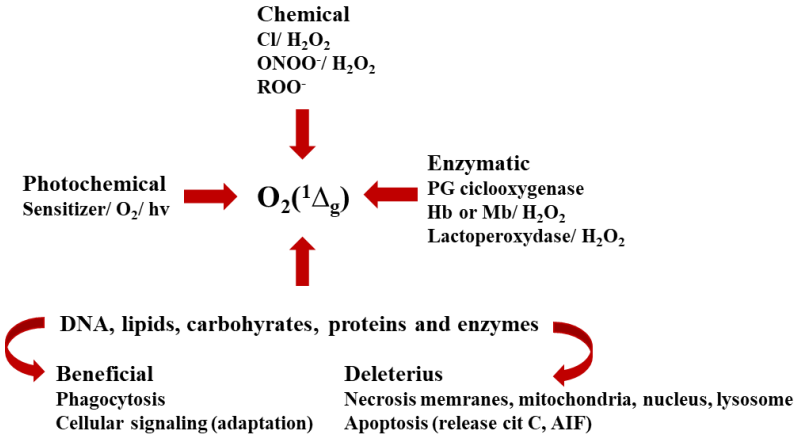

Figure 6: Schematic representation of targets, sources and biological responses of singlet oxygen [53].

$^1O_2$ has very short lifetime and the magnitude of that lifetime depends on the solvent characteristics. For instance, lifetime values were obtained as 73 ms in carbon tetrachloride which is the longest, 3.3 μs in water and 101 μs in dichloromethane according to the literature [54].

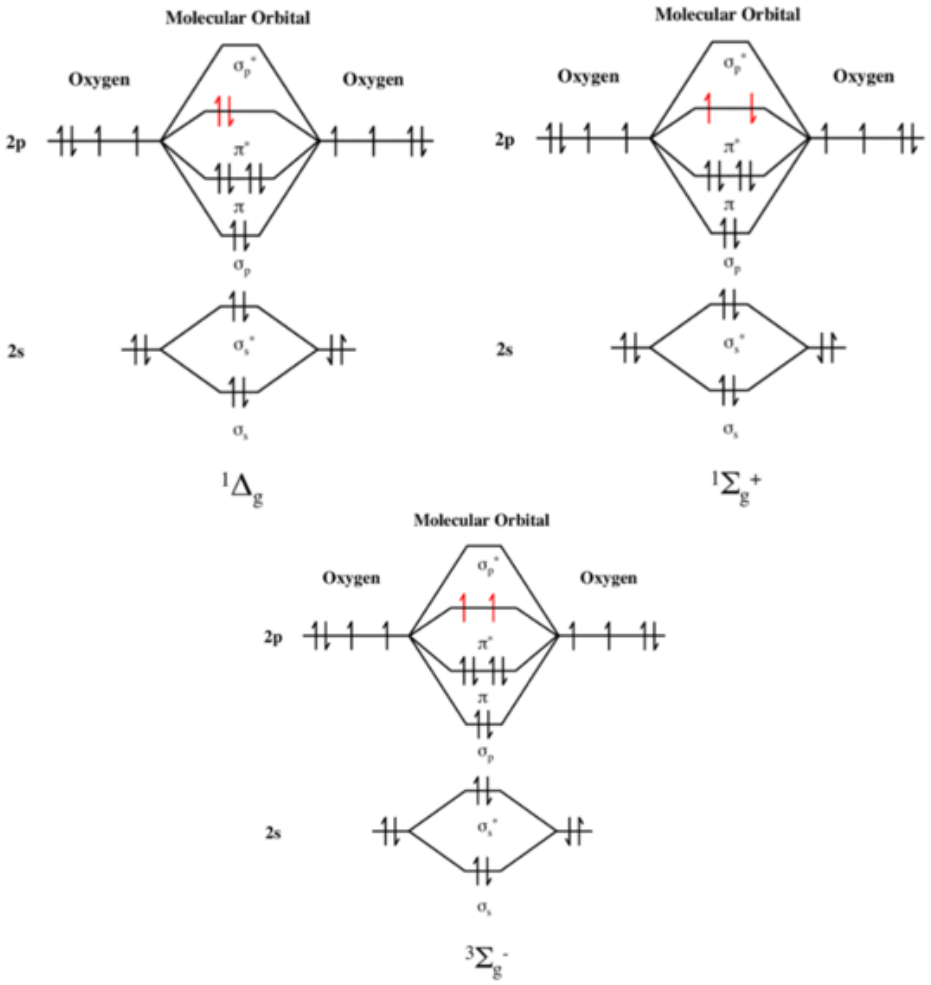

Figure 7: Molecular orbital diagrams of two excited states $^1\Delta_g$ & $^1\Sigma_g^+$ and triplet ground state $^3\Sigma_g^-$ of oxygen [56].

The electronic structure of excited and ground state of oxygen molecules should be considered to be able to understand the nature of singlet oxygen. As it was mentioned earlier, there are two types of oxygen: singlet oxygen and

molecular (triplet) oxygen. Molecular oxygen ($^3\Sigma_g^-$) with two unpaired electrons which are distributed in the highest occupied orbitals has two singlet excited states which are $^1\Delta_g$ and $^1\Sigma_g^+$ due to the rearrangement of the electron spins within these two degenerate orbitals [55]. The corresponding molecular orbitals are represented in the **Figure 7** [56].

In previous researches, it was found that $^1\Delta_g$ has 22.5 kcal/ mol^{-1}, $^1\Sigma_g^+$ has 31.5 kcal / mol^{-1} energy higher than the triplet state, $^3\Sigma_g^-$ [57]. For the $^1\Delta_g$ singlet state, both electrons are paired in just one orbital and the other one is vacant which is expected to undergo two–electron reactions, whereas the spin pairing electrons are in different orbitals which is expected to undergo one – electron free radical reactions for the $^1\Sigma_g^+$ singlet state [58].

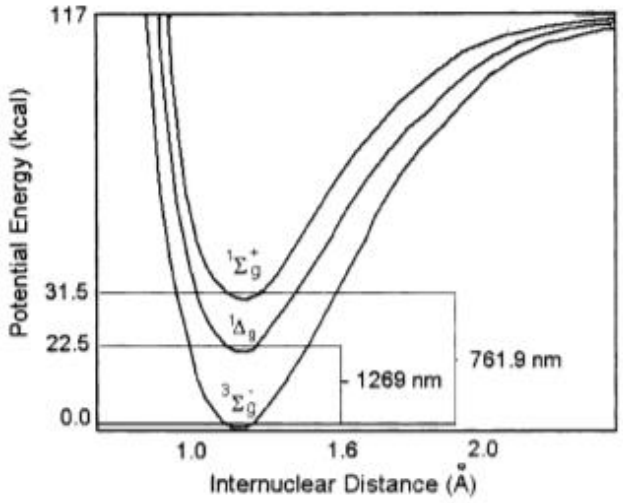

Figure 8: Potential energy diagram of three electronic states of molecular oxygen that was mentioned. Reprinted with permission from reference [56] Copyright © (2002) Elsevier.

The differences between two excited states arise from the change in π-antibonding orbitals [56]. $^1\Delta_g$ has longer lifetime compared to $^1\Sigma_g^+$ since the transition is spin forbidden for $^1\Delta_g$ to $^3\Sigma_g^-$. $^1\Delta_g$ has radiative lifetime around 45 min in gas phase and 10^{-6}-10^{-3} s in solution whereas $^1\Sigma_g^+$ has 7–12 s in gas phase and 10^{-11}-10^{-9} s in solution [56]. So that is, it can undergo chemical reactions in the biological environments [59].

1.3.2. Generation & Quenching of Singlet Oxygen

There have been various ways to produce singlet oxygen over the years. The one of the first attempts for studying on the generation of singlet oxygen was accomplished by Moureu and Fritzsche independently at the beginning of twentieth century and it was based on photooxygenation of rubrene and naphthalene, respectively [60,61]. They produced singlet oxygen in a photosensitized process by exposing the sensitizer to direct sunlight in the presence of air. In the 1940's, Schenck and Ziegler proposed the first dye sensitized photooxygenation of α–terpinene, to synthesize the naturally occurring trans-annular peroxide, ascaridole by using chlorophyll as the sensitizer [62]. In the late 1950's, olefin oxidations with singlet oxygen by using the reaction of hydrogen peroxide and sodium hypochlorite was studied by Wexler and Foote [63].

It was showed that singlet oxygen can be produced by laser excitation under high pressure while 9,10-dimethyl anthracene and a singlet oxygen acceptor molecule, 1,3-diphenylisobenzofuran (DPBF) are present in the reaction

medium, in 1969 by Evans [64]. DPBF which is represented in **Figure 9** was chosen as an acceptor since it is commonly used to study the kinetics and photophysics of singlet oxygen sensitizers [38].

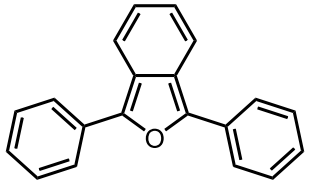

Figure 9: Structure of DPBF which is commonly used singlet oxygen trap.

Various ways are present to produce singlet oxygen and several paths can be followed by the **Figure 10** [57]. Even though, numerous different studies were introduced to generate singlet oxygen, two methods are accepted as the most common ways which are photosensitization and chemical means also known as Type I and II reactions. Since the yield of chemically produced singlet oxygen is limited by the stoichiometry of the reaction which can also result in unreacted material or side product, photosensitization of the ground state oxygen is often chosen compared to chemical synthesis methods.

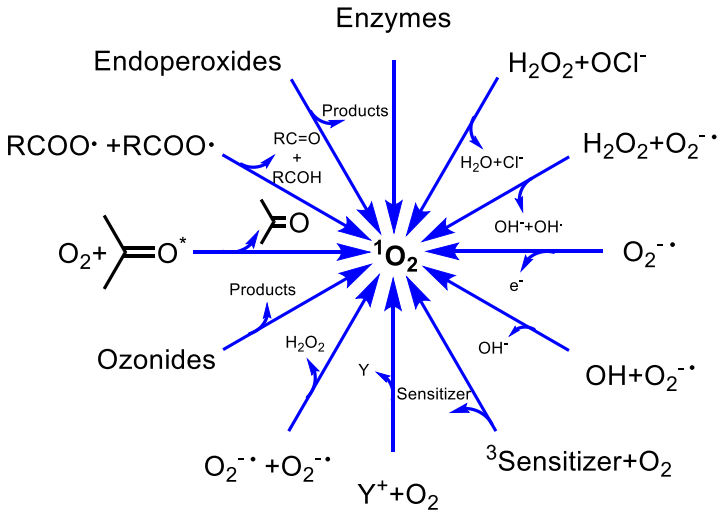

Figure 10: Schematic representation of different paths to produce singlet oxygen [6].

Photosensitized generation of singlet oxygen is admitted as the simplest and most controllable way [56] and this method requires only the presence of light at appropriate wavelength, a photosensitizer and oxygen as it was mentioned in previous chapters. When the light is absorbed by the photosensitizer, PS goes into its excited state and transfers its energy to molecular oxygen to generate singlet oxygen. The visual explanation for this statement can be seen in **Figure 11.**

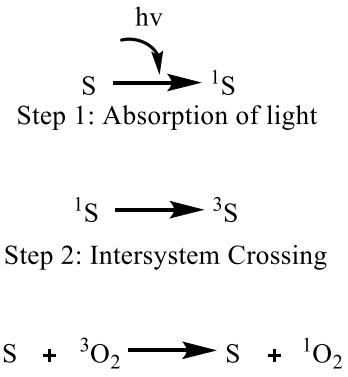

Figure 11: Schematic representation of the process of PS excitation and $^1O_2$ generation.

Singlet oxygen can also be generated naturally in living organisms and plants, and is a problem in the photodegradation of polymers [65,66].

1.3.3. Application of Photosensitized Singlet Oxygen

Reactions of singlet oxygen might generate toxic products or might cause changes in DNA strands and bases. However, the reactivity of singlet oxygen can become not only harmful but also beneficial such as signaling molecule when it is used at low concentrations [59]. Also, due to the versatility and high

degree of stereoselectivity of singlet oxygen, it becomes a useful synthetic reagent to synthesis of fine chemicals or to treat wastewater [56]. The generation of singlet oxygen around a diseased tissue such as tumor can enable cell death and behave as a therapeutic agent against cancers, skin diseases and macular degeneration [67].

1.4. Singlet Oxygen Delivery Systems

Singlet oxygen is not inevitably produced by the help of a photosensitizer in the cell because the applications of photosensitization have its own limitations. It suffers from deep light penetration and the absence of enough molecular oxygen to produce cytotoxic singlet oxygen in the cancer cells as it was mentioned earlier. Therefore, reversible storage and delivery of singlet oxygen may provide a viable alternative to photosensitized generation of singlet oxygen [68]. Aromatic endoperoxides may offer a reasonable storage and delivery path [69].

The stability of the endoperoxides differ widely, but at least in a large number of 2-pyridone, naphthalene and anthracene endoperoxides, clean and high yield release of singlet oxygen was clearly documented [70]. Release of singlet oxygen in cancer cell cultures were shown to induce apoptotic response [44].

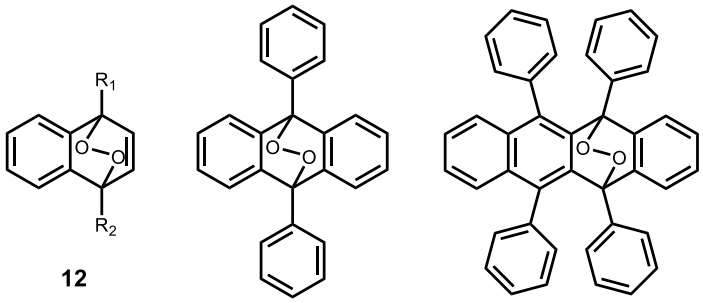

Figure 12: Examples of polycyclic aromatic endoperoxides

1.4.1. Preparation of Endoperoxides

Storage of singlet oxygen can be achieved by generating electron rich aromatic systems which are called endoperoxides. Singlet oxygen can form endoperoxides by undergoing different type of reactions and two of these reactions are admitted especially important. It can be produced by the addition to olefins to form allylic hydroperoxides or the addition to diene system to form endoperoxides that are related to Diels-Alder reactions [71]. Mostly, they are prepared by photosensitized oxygenation which occurs [4+2] cycloaddition of singlet oxygen on the electron rich carbons of the aromatic substrate. Even though, it seems it has a concerted mechanism like in the case of Diels-Alder reaction, yet it cannot be accepted as the same. As it is shown in **Figure 13**, endoperoxide can be formed in a concerted matter which can be called chemical quenching or it undergoes spin-forbidden intersystem crossing to yield a complex at triplet state which dissociates to triplet oxygen and an aromatic ring which can be called physical quenching [72, 73].

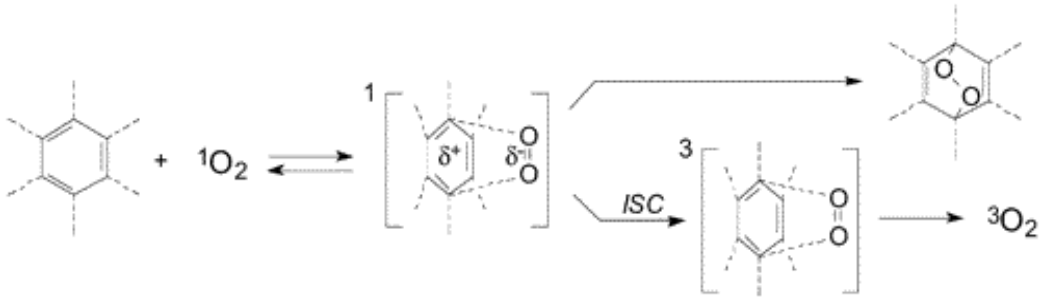

Figure 13: Endoperoxide formation mechanism by [4+2] cycloaddition of singlet oxygen on aromatic hydrocarbons. Reprinted with permission from reference [73] Copyright © (2003) American Chemical Society.

Storage of singlet oxygen on endoperoxides show several differences based on steric and electronic effects. The reactivity of aromatic hydrocarbons increases with the increasing number of the electron donating groups involved since singlet oxygen has strong electrophilicity. The rate order to undergo reaction for various groups attached to aromatic structures such as H< C_6H_6< CH_3< OCH_3 can be given as an example [73].

The number of fused rings can be considered as another significant parameter. Molecules that possess more than two rings such as anthracene or tetracene showed the reactivity increases two-fold when the number of fused rings increases [74].

Steric effect might diversify depending on the structure of aromatic substrate, therefore several cases should be analyzed to have a better insight. Regioselectivity of the cycloaddition may alter according to the steric hindrance. For instance, severe strain on the structure can be relieved when singlet oxygen is added to the structure to synthesize endoperoxide for the compound known as Heli-anthracene (HEL) which is seen in **Figure 14** [73].

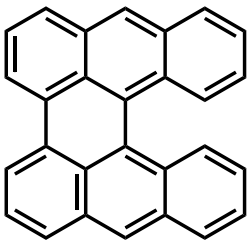

15

Figure 14: Heli-anthracene (HEL)

Additionally, in the case of 1,8-dimethylnaphthalene in **Figure 15**, steric strain is released in the transition state by the aid of neighboring two methyl groups bound to polycyclic aromatic hydrocarbon which increases the reaction rate. 1,8-dimethylnaphthalene is 4 times more reactive compared to 1,5-isomer due to these close methyl groups [75].

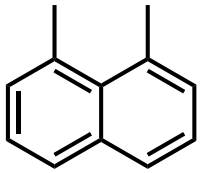

16

Figure 15: The proximity of the methyl groups in 1,8-dimethylnaphthalene alters the reaction rates.

The synthesis of endoperoxides is strongly dependent on solvent properties for [4+2] cycloadditions compared to regular Diels-Alder reactions. More detailed investigation about singlet oxygen cycloaddition of cyclic 1,3-dienes was performed by using 28 different solvents [76]. The study was majorly based on the solvent impact on reaction rate of singlet oxygen quenching by 1,4-dimethylnaphthalene and it was revealed that the rate has increased from cyclohexane to formamide. In addition, the overall rate becomes even much higher with the water-soluble analogs.

1.4.2. Dissociation of Endoperoxides

Endoperoxides can dissociate in two main pathways which are thermolysis and photolysis. Both pathways include two different mechanisms: Cycloreversion leading to the parent substrate and oxygen either in singlet or triplet state and homolytic cleavage of the peroxide bond often followed by decomposition or rearrangement as seen in **Figure 16** [73].

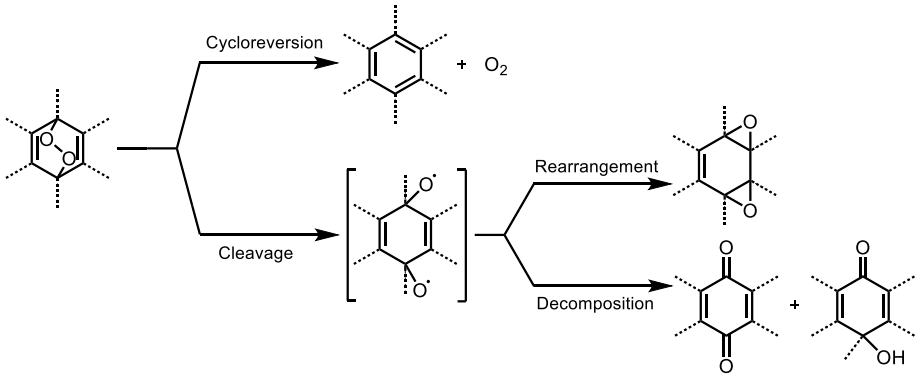

Figure 16: Dissociation pathways for polycyclic aromatic endoperoxides. Reprinted with permission from reference [73] Copyright © (2003) American Chemical Society.

In the case of concerted cycloreversion, singlet oxygen is generated. On the other hand, diradicals which are formed by cleavage leads to both singlet and triplet oxygen. As in the following **Figure 17**, obtained singlet state diradicals firstly form singlet oxygen, however, some of these might turn into triplet oxygen by intersystem crossing [77].

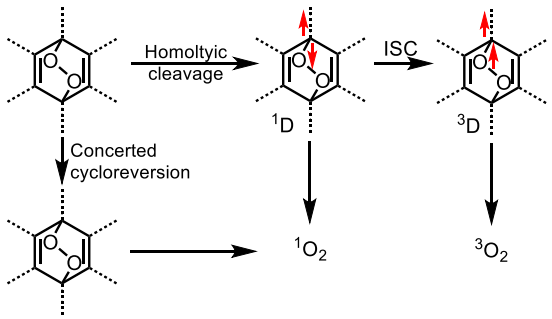

Figure 17: Competing pathways for the release of singlet oxygen from endoperoxides [73]

Several types of polycyclic aromatic endoperoxides were shortly mentioned earlier. Aubry and her colleagues have reported that the activation enthalpy for cycloreversion ascends from benzene derived to naphthalene and 1,4- anthracene derived endoperoxides. Additionally, it was stated that cycloreversion competes with homolytic cleavage when more condensed equivalent derivatives are considered and the possibility to undergo cycloreversion is more likely if the aromatic substituents at the bridgehead meso positions are present [73]. These explanations can be proved by looking specifically 8-10, 11c/12a, 22c/22e in **Figure 18** and **Figure 19.**

Endo**P**er**O**xide		ΔH (kJmol^{-1})	ΔS (JK^{-1}mol^{-1})	$^1O_2$ (%)
	**8**	74.4±2	–1.7±8	90±3
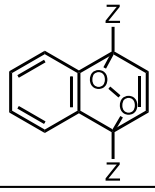	**9a**	97.0±4	0.8±5	≈100
	9b	101.1±1	8.4±4	76±1
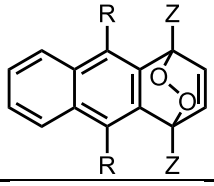	**10d**	124.6±1	–7.5±3	92±1
	10e	101.1±1	–1.3±3	95±5
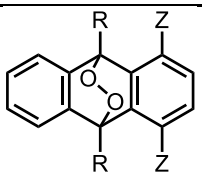	**11c**	135.8±1	40.1±2	32±1
	11d	132.9±1	30.9±3	52±4
a) Z=H **b)** Z=CH_3 **c)** R=C_6H_5, Z=H **d)** R=C_6H_5, Z=CH_3 **e)** R=C_6H_5, Z=OCH_3 **f)** R=Z=C_6H_5				

Figure 18: Activation parameters for different cyclic endoperoxides by percentages of formation of singlet oxygen yield. Reprinted with permission from reference [73] Copyright © (2003) American Chemical Society.

Endo**P**er**O**xide		Cycloreversion (%)	Rearrangement (%)		Decomposition (%)
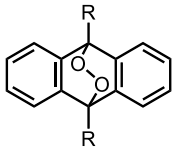	**12a**	0	80	–	6
	12b	0	5	26	17
	11c	100	–	–	–
	12d	22	46	2	19
	12f	41	33	–	3
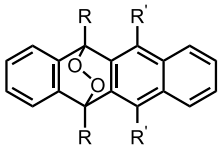	**22a**	0	10	13	40
	22c	87	–	–	–
	22d	30	50	–	–
	22e	0	22	60	–
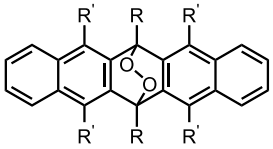	**23a**	0	–	23	41
	23d	14	35	19	–
	23e	0	55	43	–
a) R=R'=H **b)** R=R'=CH_3 **c)** R=R'=C_6H_5 **d)** R=C_6H_5, R'=H **e)** R=H, R'=C_6H_5 **f)** R=C_6H_5, R'=CH_3					

Figure 19: Yield percentages for formation of singlet oxygen by various processes after thermolysis. Reprinted with permission from reference [73] Copyright © (2003) American Chemical Society.

Cycloreversion efficiency strongly depends on temperature changes besides attached substituents or structure of the substrate. As the temperature increases, quantity of thermally activated cycloreversion generated singlet oxygen increases. Previously, the temperature dependence of anthracene endoperoxides with different substituents among all possible endoperoxides was observed by examining the UV absorptivity as a function of time [77]. The graph for 9,10-diphenylanthracene can be given in **Figure 20**.

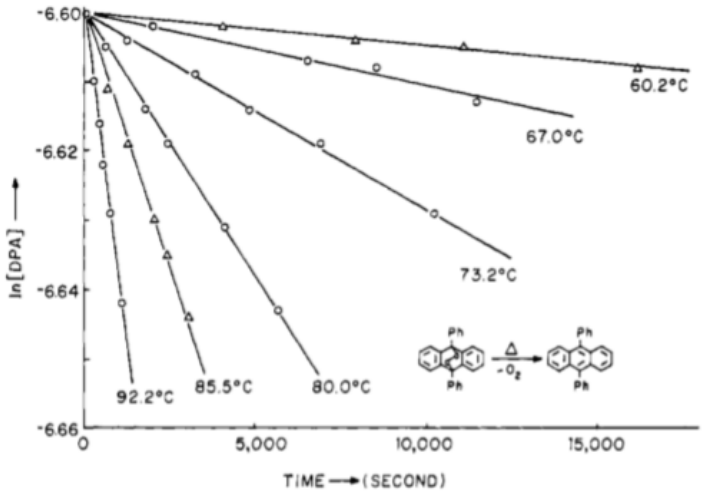

Figure 20: Temperature dependence of thermolysis of 9-10-diphenylanthracene endoperoxide to 9,10-diphenylanthracene. Reprinted with permission from reference [77] Copyright © (1981) American Chemical Society.

Supramolecular endoperoxides have also been synthesized in addition to the smaller molecules. 2,7-disulfonato-9,10-diphenyl anthracene and 2,6-disulfonato-9,10-diphenyl anthracene endoperoxides in cyclodextrins were heated between 80 and 150^{o} C and the thermal stabilities of these endoperoxides in host-guest complexes were investigated [78].

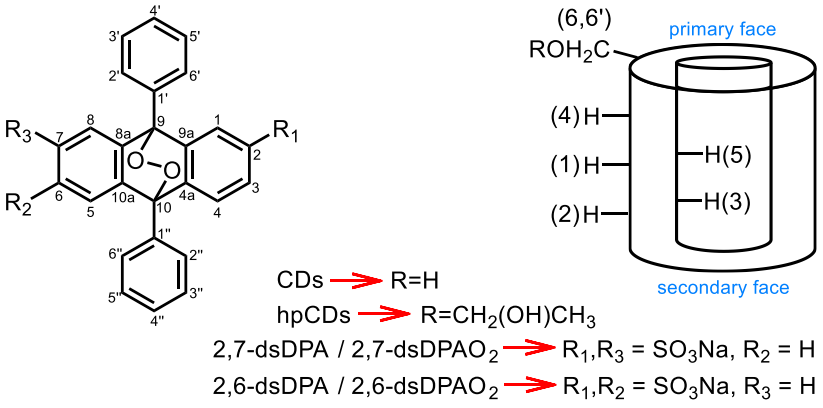

Figure 21: Schematic representations of endoperoxides, its corresponding substrates and cyclodextrins. Reprinted with permission from reference [78] Copyright © (2008) Elsevier.

System	EA (kJmol^{-1})	$t_{1/2}$ (min)			
		150°C	125°C	100°C	60°C
2,7-dsDPAO$_2$	73.3±15.3	11.0	18.6	174	2.44 x 10^4
2,7-dsDPAO$_2$/hpβCD	88.5±16.0	12.7	32.3	360	>7.50 x 10^4

Figure 22: Activation energies and thermolysis periods for supramolecular 2,7-disulfonato-9,10-diphenylanthracene endoperoxide depending on the temperature change. Reprinted with permission from reference [78] Copyright © (2008) Elsevier.

1.4.3. Singlet Oxygen Carriers

9,10-diphenyl anthracene and 1,4-dimethylnaphthalene were mentioned as singlet oxygen storage and delivery units without giving detailed information in previous chapters. Kinetic stability of endoperoxides around 30-40^0 C (around human body temperature) is very significant for disease treatments. 9,10-anthracene derivatives fulfill this aim perfectly and when heated it can undergo cycloreversion very easily. According to Akkaya et al., these 9,10-anthracene endoperoxides connected to gold nanorods can store singlet oxygen at RT typically for years and release it by heating the nanorods at 808 nm light [51].

1,4-dimethylnaphthalene is counted as another type of singlet oxygen carrier. Since it is chemically stable, commercially very available and reacts relatively rapid with singlet oxygen, it is chosen commonly in photodynamic therapy applications. 1,4-dimethylnaphthalene endoperoxides can dissociate at room temperature with half-life around 5 hours. So, it can be said that gentle and

small amount of warming becomes fairly enough to release singlet oxygen that is stored in the structure [79]. Next, the research groups of Saito et al. and Nieuwni et al. have started to synthesize water soluble naphthalene derivatives like the ones in **Figure 23** and utilize as singlet oxygen delivery in biological environment [80,81].

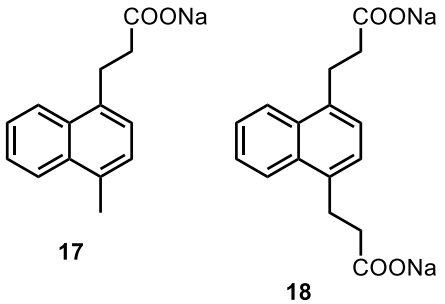

Figure 23: First examples of water-soluble naphthalene derivatives to carry singlet oxygen.

Matsumoto et al. has reported 2-pyridone also as a singlet oxygen storage unit almost recently. N-substituted 2-pyridones can release singlet oxygen with efficiency higher than 80%, while benzyl substituted 2-pyridone can release with 96% and 81% efficiency at low and high conversion rates, respectively [82]. Furthermore, N-pyridones is taught to be better for biological applications owing to its decomposition at lower temperatures compared to anthracene endoperoxides. 2-pyridone endoperoxides were introduced in photodynamic therapy [83] and synthetic applications [84]. Some 2-pyridone derivatives are used to avoid cell deaths in some tissue engineering applications when the molecular oxygen is supplied. Because these pyridones release singlet oxygen but not triplet oxygen and undergo retro Diels-Alder type reactions, some singlet

oxygen quenchers are used [85].

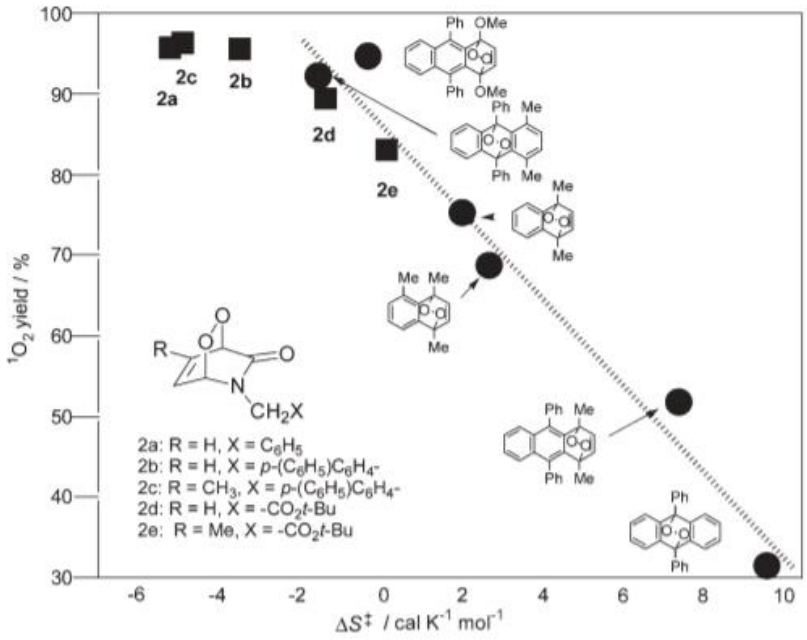

Figure 24: Comparison of singlet oxygen generation yield and activation entropy between pyridone and other polycyclic aromatic endoperoxides. Reprinted with permission from reference [82] Copyright © (2005) Royal Society of Chemistry.

CHAPTER II

Experimental Procedures

2.1 General Procedures

All chemicals and reaction solvents purchased from Sigma Aldrich, Acros Organics and ABCR were used without purification. Flash column chromatography (FCC) purifications were performed with glass columns using Merck Silica gel 60 (particle size: 0.040-0.063 mm, 230-400 mesh ASTM) and reactions were monitored by thin layer chromatography (TLC) using precoated silica gel plates (Merck Silica Gel PF-254) and visualized by UV light. Chromatography solvents (DCM, n-hexane, EtOAc) were purchased as technical grade and were purified employing fractional distillation before use. All organic solutions after extraction were dried over anhydrous Na_2SO_4 and concentrated by using rotary evaporator before being subjected to flash column chromatography (FCC). Anhydrous THF was used freshly after refluxing over Na in the presence of benzophenone under Ar.

^{1}H and ^{13}C NMR spectra were recorded on Bruker Spectrospin Avance DPX 400 spectrometer (operating at 400 MHz for ^{1}H NMR and 100 MHz for ^{13}C NMR) using deuterated solvents ($CDCl_3$, DMSO-d_6) with tetramethylsilane (TMS) as internal standard purchased from Merck and chemical shifts are reported in ppm values. Spin multiplicities are reported as following: s (singlet), d (doublet), t (triplet), q (quartet), quint (quintet), sext (sextet), dd (doublet of doublets), dt (doublet of triplets), td (triplet of doublets), m (multiplet), bs (broad signal). High Resolution Mass Spectroscopy (HRMS) experiments were done on an Agilent Technologies-6530 Accurate-Mass Q-TOF-LC/MS. The thermogravimetric analysis (TGA) was performed with TA – Q500 TGA.

2.2 Synthesis Scheme

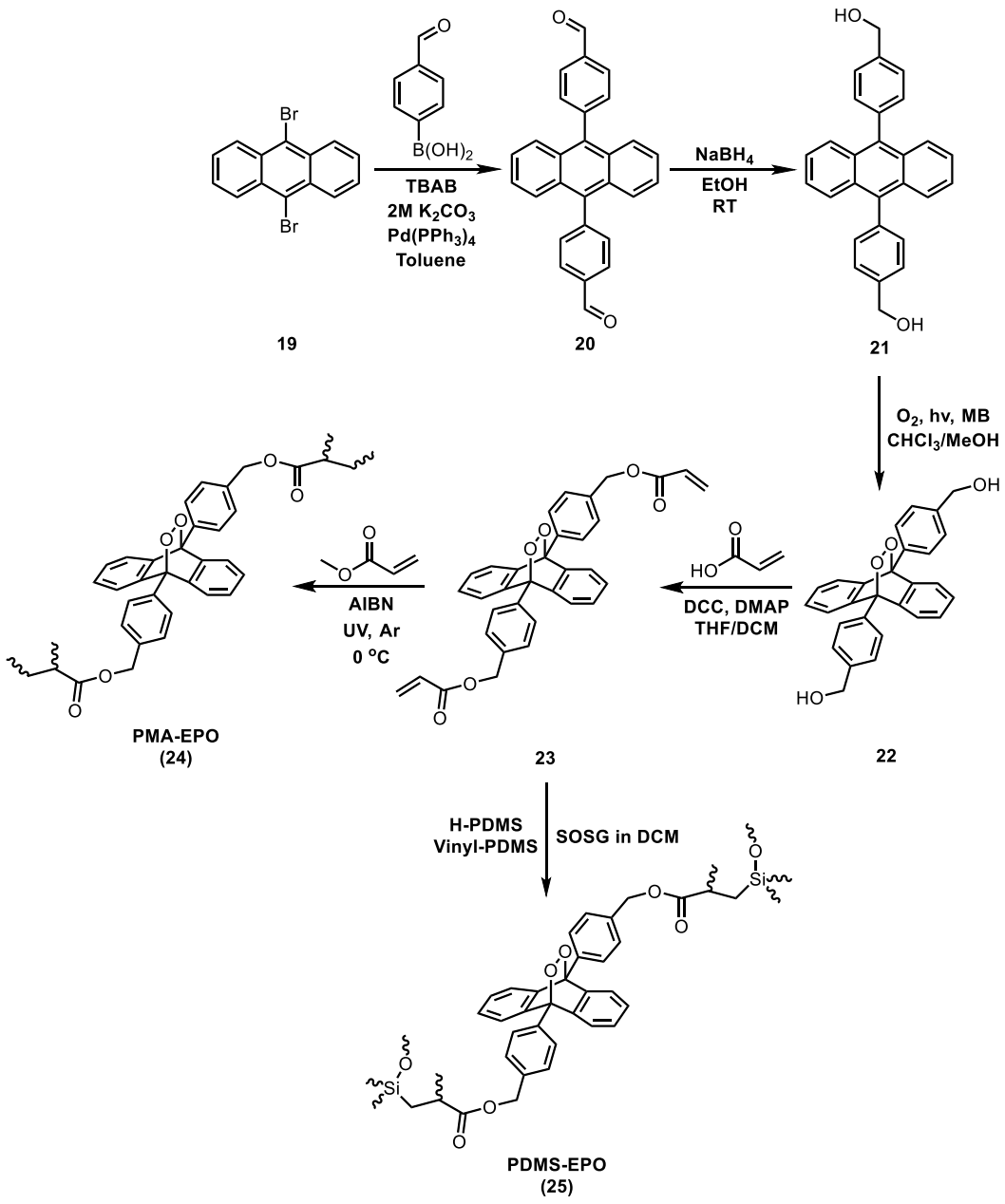

Scheme 1: Synthesis scheme of PMA-EPO **(24)** and PDMS-EPO **(25).**

2.2. 1 Synthesis of Compound 20

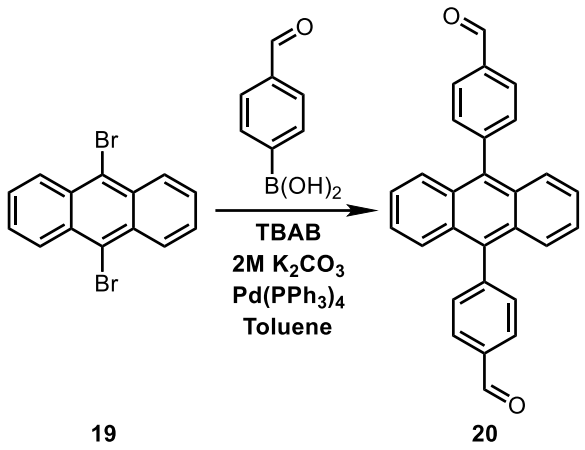

Figure 25: Synthesis of compound **20**

9,10-Dibromoanthracene (0.50 g, 1.50 mmol) and 4-formylphenylboronic acid (0.54 g, 3.57 mmol) were dissolved in the toluene (10 ml). TBAB (2 mg, cat.) and 2M $K_2CO_{3(aq)}$ solution (3.2 ml) was added to the reaction mixture and the mixture was stirred at room temperature for 30 min under Ar. Then, $Pd(PPh_3)_4$ (2 mg, cat.) was added to the mixture and refluxed at 90°C for 24 h. The mixture was poured into water and extracted with DCM. The organic layer was dried over anhydrous sodium sulfate and the solvent was removed under reduced pressure. The residue was purified by column chromatography over silica gel with hexane, and then followed by DCM as eluent. Compound **20** was obtained as yellow solid (0.35 g, 61%).

^{1}H NMR (400 MHz, $CDCl_3$): δ 10.24 (s, 2H), 8.18 (d, J= 8.1 Hz, 4H), 7.71 (d, J= 8.1 Hz, 4H), 7.68-7.60 (m, 4H), 7.43-7.37 (m, 4H). ^{13}C NMR (100 MHz, $CDCl_3$): δ 192.0, 145.8, 136.2, 135.8, 132.1, 129.9, 129.4, 126.5, 125.7.

2.2.2 Synthesis of Compound 21

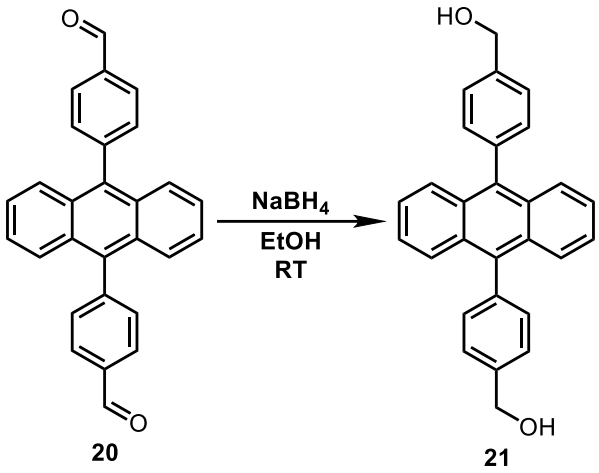

Figure 26: Synthesis of compound **21**

Compound **20** (0.33 g, 0.86 mmol) was suspended in 5 ml ethanol. Sodium borohydride (0.03g, 0.86 mmol) was added to the suspension and the resulting mixture was stirred for 30 min at room temperature. Then, the reaction mixture was quenched with water and extracted with diethyl ether. The organic layer was dried over anhydrous sodium sulfate and the solvent was removed under reduced pressure. The residue was purified with column chromatography over silica gel with DCM as eluent. Compound **21** was obtained as pale-yellow solid (0.85 g, 99%).

^{1}H NMR (400 MHz, DMSO-d_6): δ 7.65-7.57 (m, 8H), 7.45-7.37 (m, 8H), 5.36 (t, J=5.7 Hz, 2H), 4.71 (d, J=5.7 Hz, 4H). ^{13}C NMR (100 MHz, DMSO-d_6): δ 142.5, 137.0, 136.9, 131.1, 129.8, 127.2, 126.9, 125.9, 63.3.

2.2.3 Synthesis of Compound 22

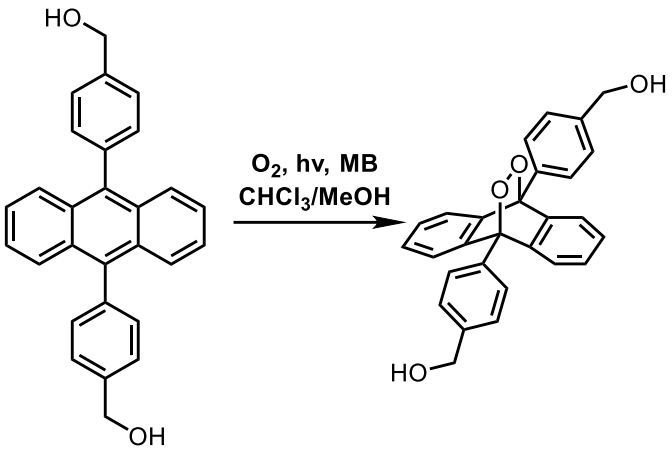

Figure 27: Synthesis of compound **22**

Compound **21** (0.20 g, 0,51 mmol) was dissolved in the mixture of $CHCl_3$/MeOH (20:5 ml) and cooled in ice bath. A pinch of methylene blue was added to the solution, and the mixture was irradiated with halogen lamp (500W) while O_2(g) was passing through the system for 2 hr. The progress of reaction was monitored with TLC (eluent:EtOAc). After removal of the solvent under reduced pressure, the residue was purified with column chromatography over silica gel with EtOAc as eluent. Compound **22** was obtained as white solid (0.13 g, 60%).

^{1}H NMR (400 MHz, DMSO-d_6): δ 7.65 (d, J=8.1 Hz, 4H), 7.59 (d, J=8.1 Hz, 4H), 7.33-7.27 (m, 4H), 7.12-7.05 (m, 4H), 5.38 (t, J=5.7 Hz, 2H), 4.68 (d, J=5.7 Hz, 4H). ^{13}C NMR (100 MHz, DMSO-d_6): δ 143.3, 140.4, 131.0, 128.3, 127.3, 127.0, 123.5, 83.8, 63.1.

2.2.4 Synthesis of Compound 23

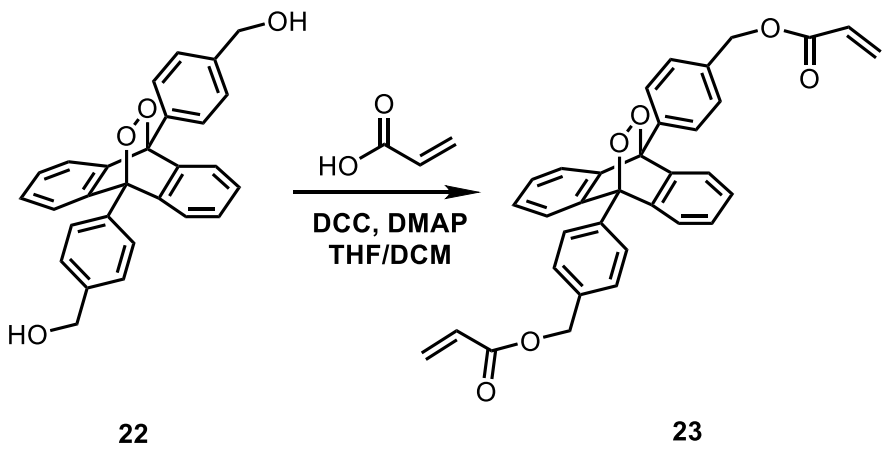

22 **23**

Figure 28: Synthesis of compound **23**

Compound **22** (0.30 g, 0,72 mmol), DCC (0.59 g, 2.85 mmol), DMAP (0.03 g, 0.21 mmol), and acrylic acid (0.20 mL, 2.85 mmol) were dissolved in mixture of dry THF/DCM (8:60 ml) and the slurry mixture was stirred at room temperature for 24 hr under Ar. The DCU was removed by vacuum filtation and the filtrate was collected. The solvent was removed under reduced pressure and the residue was purified with column chromatography over silica gel with DCM as eluent. Compound **23** was obtained as yellow solid (0.14 g, 38%).

^{1}H NMR (400 MHz, $CDCl_3$): δ 7.74 (d, J=8.4 Hz, 4H), 7.67 (d, J=8.4 Hz, 4H), 7.26-7.22 (m, 4H), 7.22-7.17 (m, 4H), 6.57 (dd, J= 17.3 Hz, J= 1.4 Hz, 2H), 6.29 (dd, J=17.3 Hz, J=10.4 Hz, 2H), 5.95 (dd, J= 1.4 Hz, J=10.4 Hz, 2H). ^{13}C NMR (100 MHz, $CDCl_3$): δ 166.1, 140.1, 136.1, 133.0, 131.4, 128.3, 128.0, 127.8, 127.7, 123.5, 84.1, 65.9.

2.2.5 Synthesis of PMA-EPO (anthracene-endoperoxide polymethacrylate copolymer) (24) (Free Radical Polymerization)

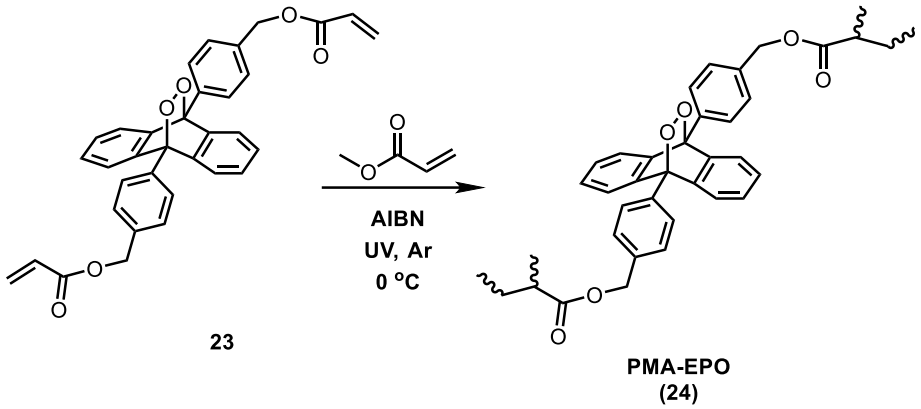

Figure 29: Synthesis of **PMA-EPO (24)**

Compound **23** (22 mg 0.04 mmol) was dissolved in methyl acrylate (1 mL) under an Ar atmosphere and then, AIBN (4 mg) was added to the solution and well mixed again under Ar atmosphere. The resulting mixture was added to the mold covered with a glass plate. The mold was irradiated with UV light while cooling in an ice bath for 30 min. The resulting polymer was extracted with THF (3 x 200 mL) over 24 hr. Then, the polymer was dried under vacuum for 3 hours. PMA-EPO was obtained as transparent solid.

2.2.6 Synthesis of PDMS-EPO (elastomeric poly(dimethylsiloxane) (25)

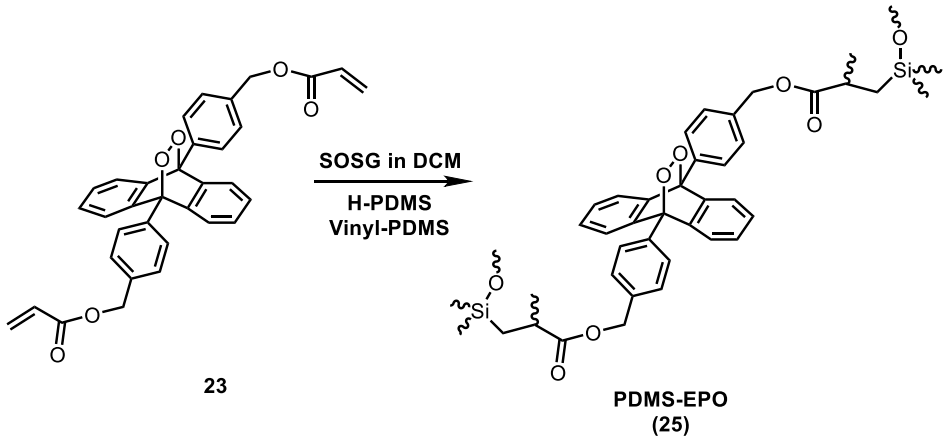

Figure 30: Synthesis of **PDMS-EPO (25)**

Sylgard® 184 that is a patented two-part (Base (10.0 g) and Curing Agent (1.0 g)) was mixed in 10:1 ratio in a plastic vessel with a wood stirrer until whitish colored foam is seen (At least 2-3 min is a necessity). Compound **23** (75 mg, 0.14 mmol) which was previously dissolved in DCM (0.5 mL) was mixed with whitish foam Sylgard® 184 until complete dissolution is established. The resulting mixture was separated into two different plastic petri dishes (5.0 g & 5.0 g). SOSG (0.2 mL) that was dissolved in DCM (0.5 mL) was added into the second petri dish and blended thoroughly. Both petri dishes were put in vacuum desiccator and vacuum pump was operated for 1 hr. Then, petri dishes were left stand untouched next 2 days at RT. Once cured, the films were peeled away and cut into strips for testing.

2.3. Mechanochemical Generation of Singlet Oxygen from PMA-EPO

2.3.1. Preparation of singlet oxygen sensor solutions

A stock solution of Singlet Oxygen Sensor Green Reagent (100 μg, S36002, Molecular Probes), which is highly selective towards singlet oxygen in presence of radical species such as OH and superoxide radicals (common mechanochemical products of polymer degradation) was prepared as follows: Argon gas was bubbled through 33 mL of methanol to remove any dissolved oxygen. 100μg of singlet oxygen probe was carefully dissolved in this solvent to obtain a stock solution of 5μM. A more dilute solution (1μM) of singlet oxygen sensor was prepared by using this stock solution. Stock solution (5μM) and the

dilute solution (1μM) were separately used to probe the singlet oxygen evolved during mechanochemical reaction of PMA-EPO in the Cryomill.

2.3.2. Singlet oxygen sensing during cryomilling of PMA-EPO

3 mL (1μM or 5μM) solutions of freshly singlet oxygen solutions (vide supra) were introduced in 50 mL milling chamber (ZrO_2) of Retsch Cryomill, together with 0.240 g of PMA-EPO. Cooling time prior to milling was set as 5 min, after the chamber was cooled by liquid nitrogen, milling frequency was set to 30 Hz. The contents of the chamber were milled at this frequency for 5 and 10 min. As the control experiments, the singlet oxygen sensor solutions were milled under the same conditions but in absence of PMA-EPO.

2.4. Thermo Gravimetric Analysis Measurement

PMA-EPO was heated from 25°C to 500°C at a rate of 10°C /min under nitrogen atmosphere. TGA result indicates that the PMA-EPO has started to lose weight around 63°C and it reaches the maximum decrease in weight at temperature around 108°C.

CHAPTER III

Results and Discussion

Reversible storage and delivery of singlet oxygen is accepted as an alternative way to photosensitized generation of singlet oxygen and there is a wide range of different types of endoperoxides that may offer reasonable storage and delivery path. The stability of the endoperoxides differ widely, however, 2-pyridone, naphthalene and anthracene endoperoxides release singlet oxygen at quite high yields.

In this work, a cross-linked polyacrylate, and a PDMS elastomer incorporating anthracene-endoperoxide modules with chain extensions at the 9,10-positions were synthesized. So that, reactive oxygen species with a microsecond lifetime could be generated on a polymer support when mechanical shear forces are applied.

Kinetic stability of endoperoxides around 30-40°C (around human body temperature) is very significant for disease treatments as it was mentioned in introduction part. 9,10-anthracene derivatives fulfill this aim perfectly and when heated it can undergo cycloreversion very easily.

9,10-dibromo anthracene in **Figure 31** was chosen as the starting material due to its stability of its endoperoxide form around human body temperature Thus, our endoperoxide is optimized for treatments and it does not dissociate easily unless it is promoted.

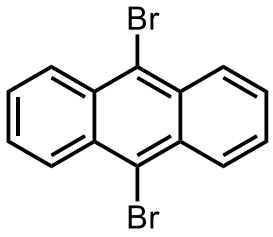

19

Figure 31: Structure of 9,10-dibromo anthracene

4,4'- (anthracene-9,10-diyl)dibenzaldehyde **20** was obtained from the C-9, 10 positions at room temperature and at 90°C, respectively, based on the principles of Suzuki coupling. The ^{1}H NMR on **Figure 44** shows the formation of an aldehyde which appears as a peak around 10.25 ppm.

Anthracene-9,10-diylbis(4,1 phenylene))dimethanol **21** was synthesized by the reduction of 4,4'-(anthracene-9,10-diyl)dibenzaldehyde **20** at room temperature. ^{1}H spectra of **20** and **21** indicates the conversion of aldehyde to

alcohol since peak at 10.25 ppm disappears while protons from OH and CH_2 groups at 5.35-5.38 ppm and 4.7 ppm are present, respectively.

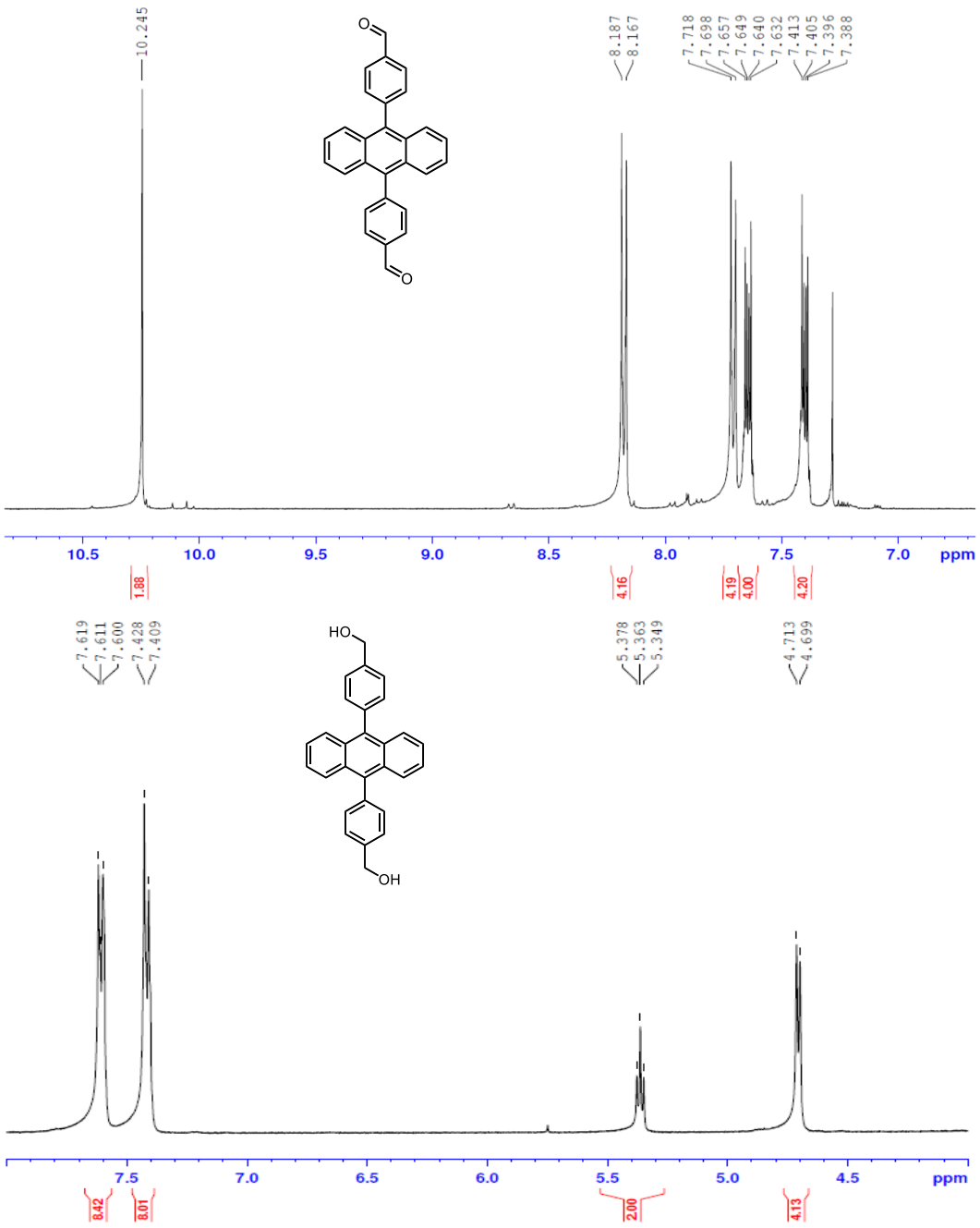

Figure 32: ^{1}H-NMR spectra of **20** and **21** with highlighted peaks.

Photosensitized singlet oxygen generation in the presence of compound **21** lead to the formation of anthracene-9,10-endoperoxide **22** was held in chloroform: methanol in -78°C which is maintained by ethanol circulation under liquid nitrogen. Methylene blue was used as our photosensitizer due to its high quantum yield and easy removal from the reaction medium once the reaction is terminated. Irradiation was achieved with a 500 W halogen lamp in the wide range. Mechanism of adding singlet oxygen to anthracene-9,10-diylbis(4,1 phenylene))dimethanol **21** is depicted on **Figure 33.**

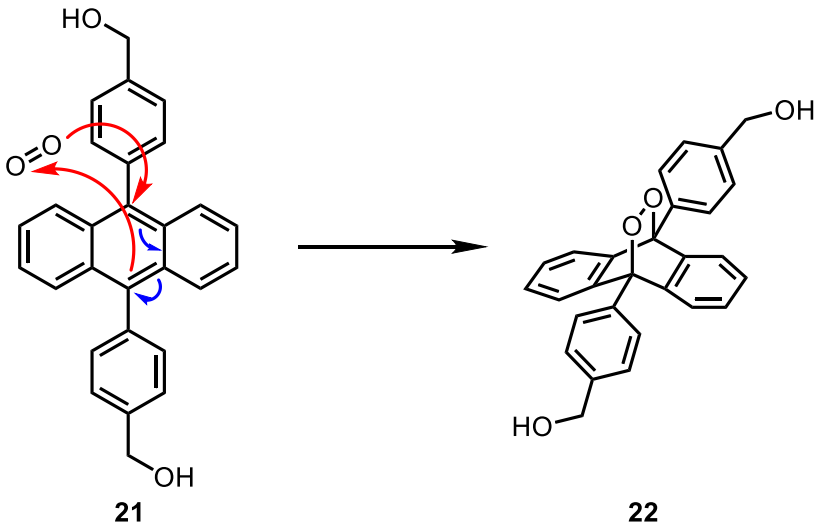

Figure 33: Mechanism of the [4+2] addition reaction of singlet oxygen to compound **21.**

The formation of anthracene-9,10-endoperoxide was confirmed as in **Figure 34** by the appearance of an additional distinct peak between 7.58 and 7.66 ppm since the symmetry of the compound has changed.

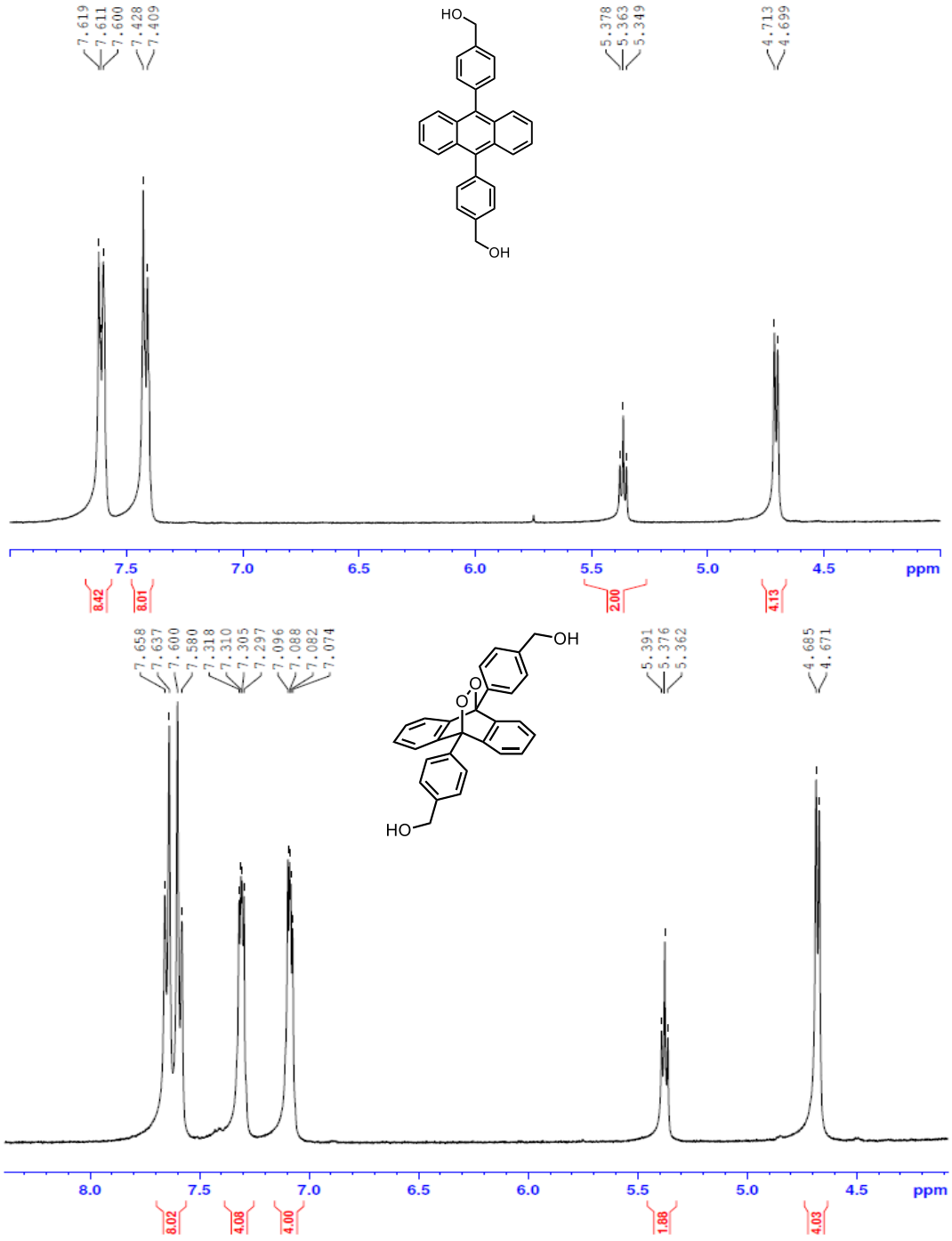

Figure 34: ^{1}H-NMR spectra of **21** and **22** with highlighted specific structural peaks.

Crosslinker of anthracene-9,10-endoperoxide **23** was targeted, once after characterization of **22** was completed. Crosslinker possess two additional CH_2 group and one CH group in each side of the compound where CH group and one of the CH_2 is double bonded to each other. Three distinct peaks at 5.95 ppm, 6.29 ppm and 6.57 ppm are seen owing to coupling on these groups.

Polymerization of the crosslinker **23** was performed to produce a cross-linked polyacrylate and a PDMS elastomer which are PMA-EPO **(24)** and PDMS-EPO **(25)**. We aimed to generate singlet oxygen from these polymer-endoperoxide derivatives by applying mechanical force instead of heating. Cryogenic ball mill was utilized to dissociate PMA-EPO, since it has the ability to minimize the possibility of thermal decomposition. Moreover, mechanochemical reactions are triggered by the high level of impact and shear forces which are produced in internally agitated ball mills around cryogenic temperatures. Before the dissociation of PMA-EPO is executed with cryogenic ball mill, PMA-EPO was heated as a control. In **Figure 35**, PMA-EPO is shown under UV light at the right and sunlight at the left. It is also seen in **Figure 36** that sample on the right is the control kept at room temperature while sample on left being exposed to heat.

Figure 35: Appearance of PMA-EPO **(24)** under UV light.

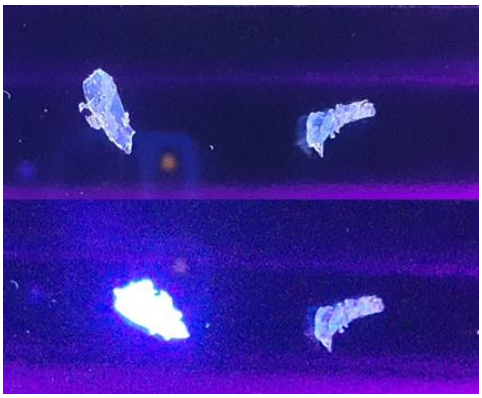

Figure 36: Thermal cycloreversion experiment with PMA-EPO **(24)**. Left column: initial form-heated form, right column: no change applied.

It was seen that singlet oxygen can be released by the thermolysis of PMA-EPO 00to its anthracene derivative and fluorescence occurs when it is heated at high temperatures (200-250°C) just for a few seconds.

After dissociation of endoperoxide and reemergence of anthracene fluorescence by heating, the preparation of singlet oxygen sensor solutions was prepared as the first step for mechanochemical generation of singlet oxygen from PMA-EPO. Singlet Oxygen Sensor Green Reagent was utilized as singlet oxygen probe since its high selectivity towards singlet oxygen in the presence of radical species [86]. Stock solution of SOSG were prepared as 5μM and it was diluted to 1μM as the second solution to probe the singlet oxygen evolved during mechanochemical reaction of PMA-EPO in the Cryomill. The contents of the chamber were milled at 30 Hz milling frequency for 5 and 10 minutes in 1μM dilute solution and 10 and 20 min in 5μM stock solution. Also, the singlet oxygen sensor solutions were milled under the same conditions without PMA-EPO as the control experiments. Emission measurements were taken under these conditions and they can be seen in the following **Figure 37** and **Figure 38**.

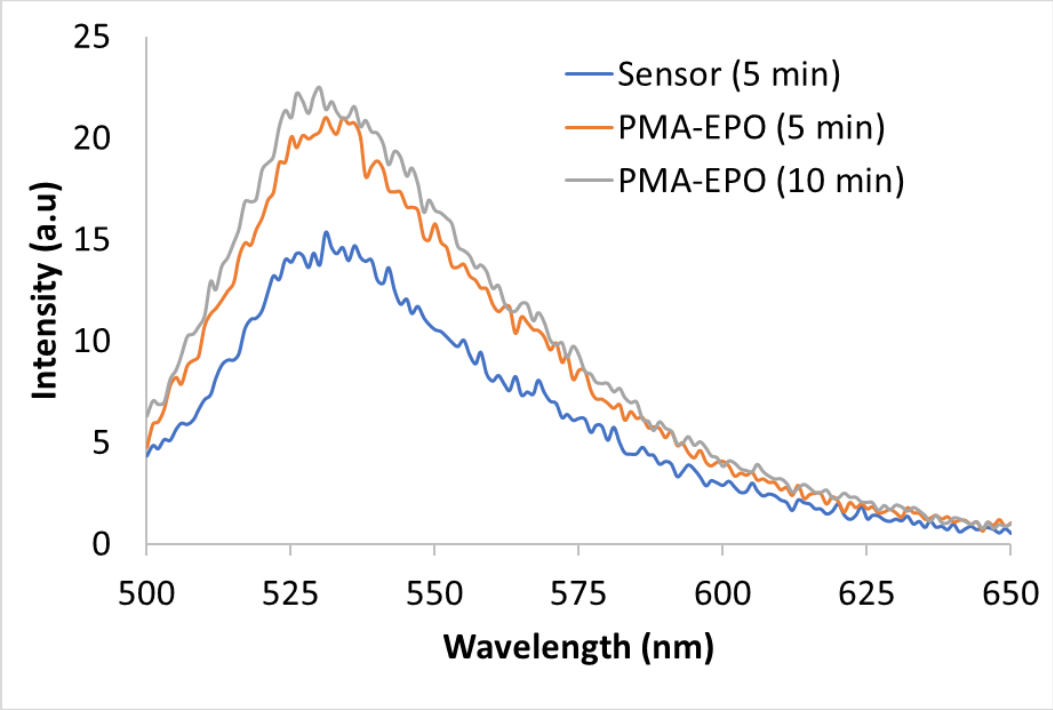

Figure 37: Fluorescence of (bottom to top); singlet oxygen sensor milled alone for 5 min, PMA-EPO **(24)** (240 mg) together with singlet oxygen sensor after 5 min, and 10 min of milling. Singlet oxygen sensor = 1 µM, 3 mL.

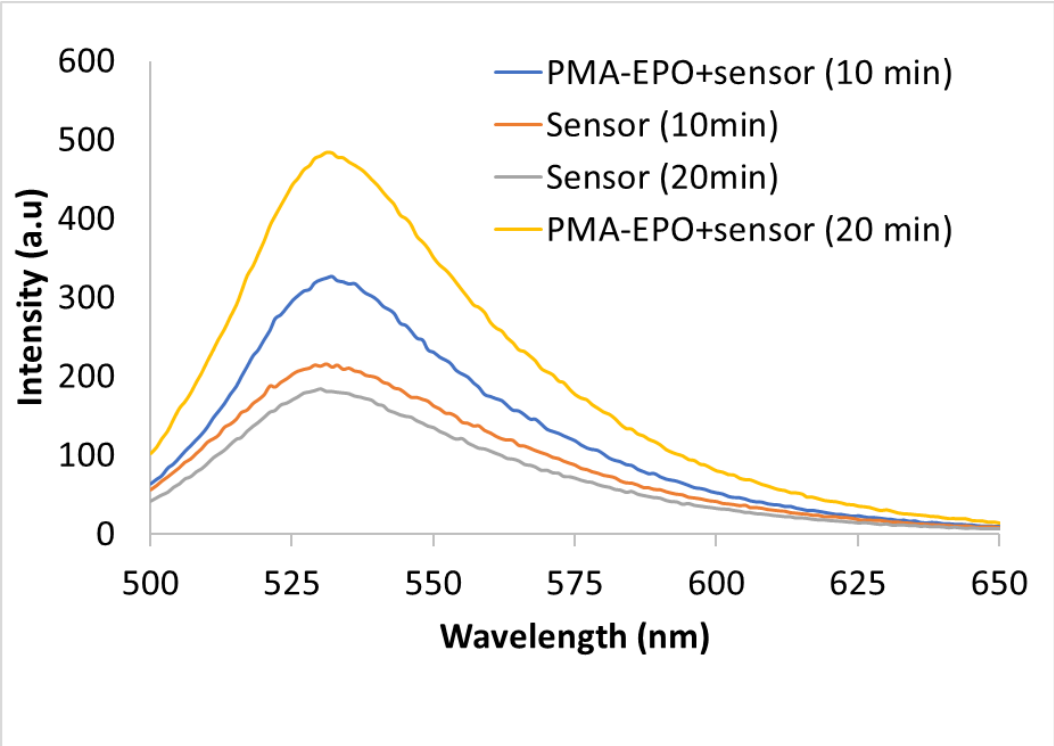

Figure 38: Fluorescence of (bottom to top); singlet oxygen sensor milled alone for 20 min, and 10 min; PMA-EPO **(24)** (240 mg) together with singlet oxygen sensor after 10 min, and 20 min of milling. Singlet oxygen sensor = 5 µM, 3 mL.

The emission spectra were measured between 500-650 nm and fluorescence value of the SOSG+PMA-EPO **(24)** has increased as the time passed from 0 to 10 min for 1 μM SOSG solution and 0 to 20 min for 5 μM SOSG solution. This result indicates that our PMA-EPO is capable of producing singlet oxygen by applying mechanochemical forces. SOSG in **Figure 39** is known as a non-florescent material in general [87]. However, when it is reacted with the singlet oxygen to produce SOSG endoperoxide, fluorescence is observed as seen in **Figure 40**. These SOSG endoperoxides are strongly fluorescent since intramolecular electron transfer (ET) is precluded. So, these findings imply that the increased fluorescence intensity is caused only from the $^1O_2$ generation of PMA-EPO.

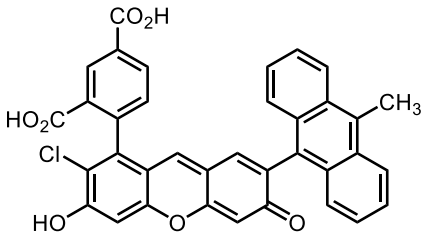

26

Figure 39: Structure of Singlet Oxygen Sensor Green® (SOSG)

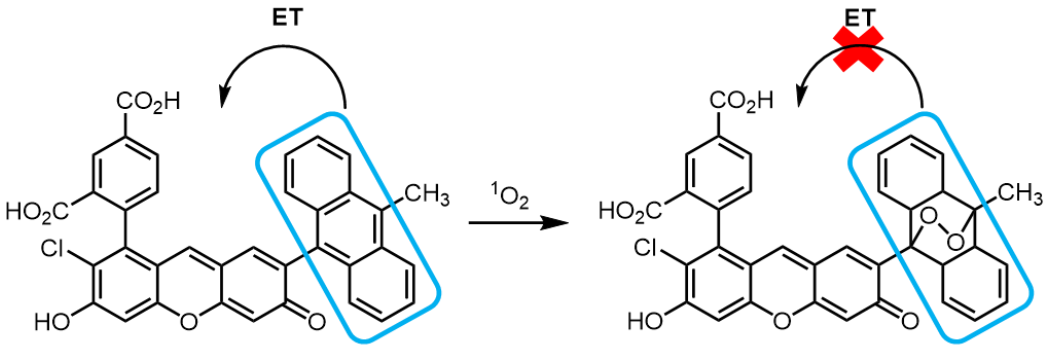

(26)
non-fluorescent SOSG

(27)
fluorescent SOSG-EPO

Figure 40: Schematic representation of the production of endoperoxide of SOSG with the reaction of SOSG and singlet oxygen [88].

For further investigation, thermogravimetric analysis was conducted, and PMA-EPO was heated from 25°C to 500°C at a rate of 10°C /min under N_2 atmosphere. TGA result shows that the PMA-EPO has started to lose weight around 63°C and it reaches the maximum decrease in weight at temperature around 108°C. As a result, there is approximately a 15% weight decreasing around 100°C, this decreasing can be correlated to the release of singlet oxygen from PMA-EPO.

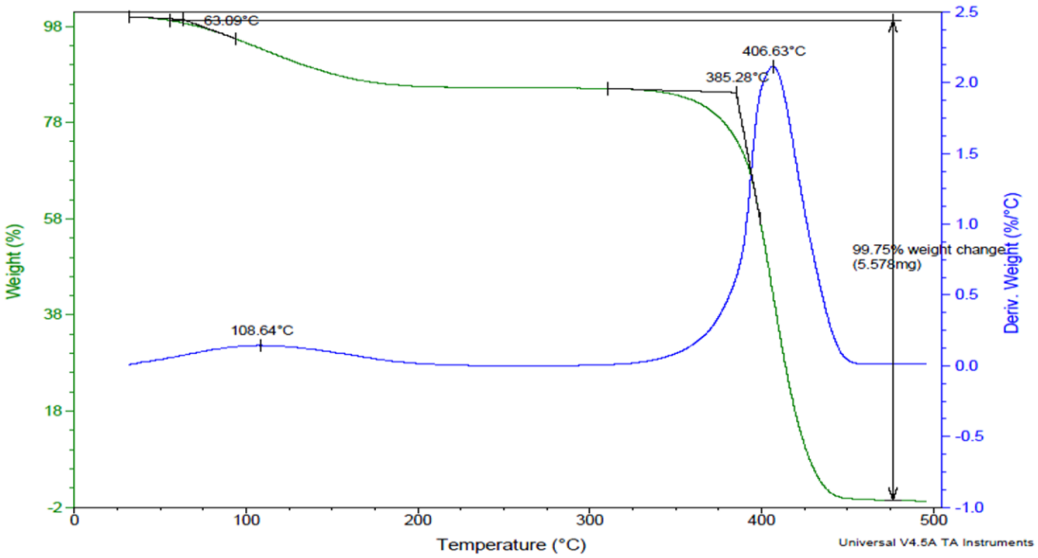

Figure 41: TGA Thermogram for PMA-EPO **(24)** with 10^0C/min heating rate under nitrogen atmosphere.

Polydimethylsiloxane (PDMS) was chosen for additional investigation since it is highly tolerant to functional groups, optically transparent and it has high mechanical strength and nearly high stretchiness [89]. Therefore, PDMS was investigated to observe the response of applying mechanochemical forces to a different type of a polymer, after PMA-EPO **(24)** has given adequate results on

mechanochemical generation of singlet oxygen according to the TGA and UV-Visible spectroscopic measurements. Mechanical force on PDMS-EPO **(25)** was applied manually as stretching and hammering. The occurrence of fluorescence was observed mostly on the sites of PDMS-EPO **(25)** that is stretched and the sites that is hammered with the possible strongest mechanical force applied. Besides, PDMS-EPO **(25)** was heated firstly to control the ability of releasing singlet oxygen and it has showed that it can dissociate to anthracene version of itself and fluoresce. As our first step, we investigated the behavior of PDMS-EPO to stretching. We have noticed that the difference between stretched strip for once and for several times is easily recognized under UV light due to increasing mechanochemical forces at the stretching sites as it can be seen in **Figure 42**.

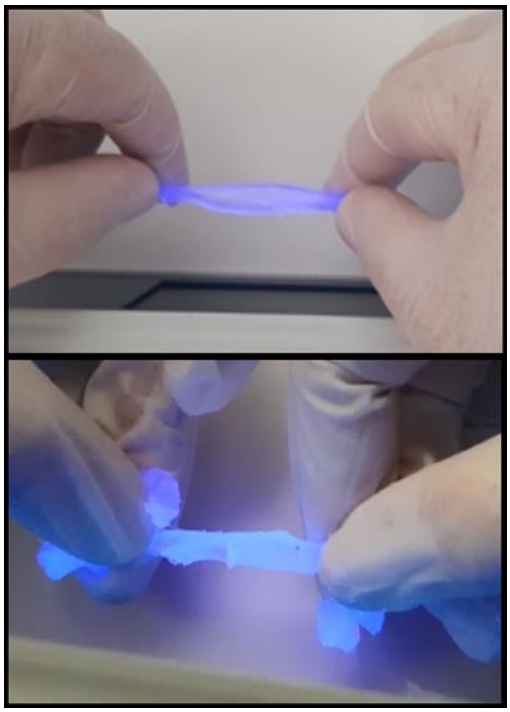

Figure 42: Two different strips of PDMS-EPO **(25)** (top to bottom); after 2 days at vacuum desiccator & stretched for once (top) and after 2 days at vacuum desiccator & stretched for several times (bottom) under UV light.

Secondly, PDMS-EPO **(25)** was hammered to see the formation of fluorescence and the change of fluorescence was examined among reference, heated PDMS-EPO **(25)** and heated for a short time period followed by hammering. These three versions of polymers are indicated in the subsequent **Figure 43**. According to the results, it can be stated that hammering has an impact on release of singlet oxygen remarkably, even tough, heating for longer time shows stronger fluorescence. More intense fluorescence is seen by hammering after 10 seconds heating compared to only heating for 10 seconds in the 1st and 2nd pictures, respectively due to the additional mechanical stress.

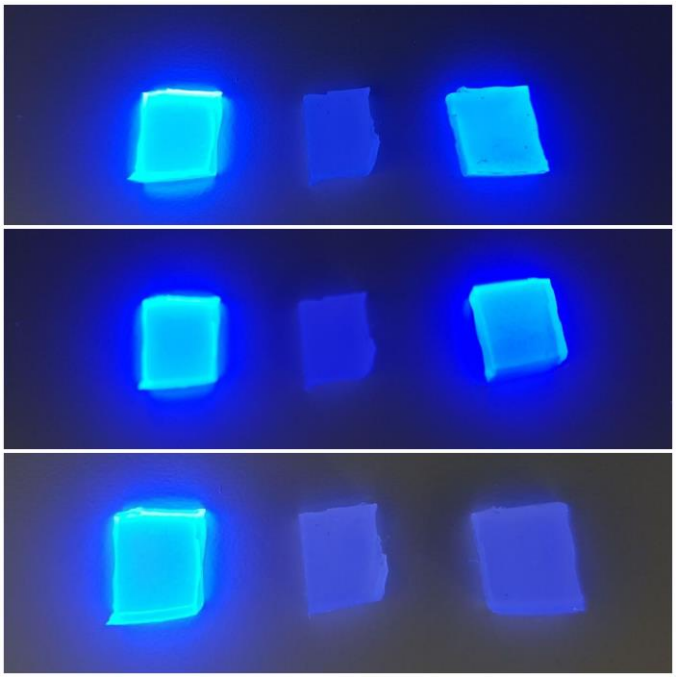

Figure 43: Three separate pieces of PDMS-EPO **(25)** under UV light (top to bottom);
Left=heated, middle=reference, right= heated for 10 sec and hammered (1st)
Left=heated, middle=reference, right=heated for 10 sec (2nd)
Left=heated, middle=reference, right=no hammering or heating (3rd).

CHAPTER IV

Conclusion

Due to many practical considerations, including cancer therapy, storage and more to the point, “controlled release” of singlet oxygen is attracting attention. The utilization of mechanochemical forces on otherwise endoperoxides to cause singlet oxygen release is a new key concept for the delivery of singlet oxygen. In this regard, the objective of this thesis was to provide proof-of-principle systems using low cost, stretchable polymers with endoperoxide tethers for the generation of singlet oxygen in a controlled manner.

Towards this goal, synthesis work was undertaken for the target monomers/crosslinkers, starting from commercially available 9,10-dibromo anthracene to the polymers which are PMA-EPO **(24)** and PDMS-EPO **(25)**. On mechanical agitation in cryogenic ball mill, enhancement of fluorescence emission of cross-linked polyacrylate PMA-EPO **(24)** was observed and assessed by spectroscopy and using a selective probe SOSG. The ability of singlet oxygen release for PMA-EPO **(24)** was also examined by TGA, and the sensitivity of

elastomer PDMS-EPO **(25)** to mechanical stress was ‘’qualitatively’’ analyzed by brute application of mechanochemical forces under UV irradiation.

This preliminary work is likely to open a path towards future studies for the quantitative assessment of mechanochemical singlet oxygen generation. One can imagine a polymeric-biocompatible strip, which could release singlet oxygen on the region where it is needed (such as melanoma) on gentle rubbing and warming by hand. Work along those lines may very well be in progress, here and abroad.

CHAPTER V

References

[1] Dolmans, D., E., J., G., J., Fukumura, D., Jain, R., K., ‘’Photodynamic therapy for cancer’’, *Nature Reviews Cancer*, 2003, 3, 380-387.

[2] Zeitouni N., C., Oseroff, A., R., Shieh, S., ‘’Photodynamic therapy for nonmelanoma skin cancers. Current review and update’’, *Molecular Immunology*, 2003, 39 (17-18), 1133-1136.

[3] Huang, Z., ‘’ A Review of Progress in Clinical Photodynamic Therapy’’, *Technology in Cancer Research & Treatment*, 2005, 4 (3), 283–293.

[4] Brown, S., B., Brown, E., A., Walker, I., ‘’The present and future role of photodynamic therapy in cancer treatment’, *The Lancet Oncology*, 2004, 5 (8), 497-508.

[5] Dougherty, T., J., Henderson, B., W., ‘’In Historical Perspective in Photodynamic Therapy’’, 1992, Maurice Dekker: New York.

[6] Dougherty, T., J., Grindey, G., B., Fiel, R., Weishaupt, K., R., Boyle, D., G., ‘’ Photoradiation therapy. II. Cure of animal tumors with hematoporphyrin and light’’, *Journal of the National Cancer Institute,* 1975, 55 (1), 115-121.

[7] Kelly, J., F., Snell, M., E., ‘’Hematoporphyrin Derivative: A Possible Aid in the Diagnosis and Therapy of Carcinoma of the Bladder’’, *The Journal of Urology,* 1976, 115 (2), 150-151.

[8] Hayata, Y., Kato, H., Okitsu, H., Kawaguchi, M., Konaka, C., ‘’Photodynamic therapy with hematoporphyrin derivative in cancer of the upper gastrointestinal tract’’, *Seminars in Surgical Oncology*, 1985, 1 (1), 1-11.

[9] Hayata, Y, et al., ‘’Hematoporphyrin Derivative and Laser Photoradiation in the Treatment of Lung Cancer’’, *Chest,* 1982, 81 (3), 269-277.

[10] McCaughan, J., S., et al., ‘’Palliation of Esophageal Malignancy with Photoradiation Therapy’’, *Cancer,* 1984, 54 (12), 2905-2910.

[11] Sandeman, D., R., ‘’Photodynamic Therapy in the Management of Malignant Gliomas: A Review’’, *Lasers in Medical Science,* 1986, 1 (3), 163-174.

[12] Hill, J., S., et al., ‘’Selective Uptake of Hematoporphyrin Derivative into Human Cerebral Glioma’’, *Neurosurgery*, 1990, 26 (2), 248-254.

[13] Popovic, E., A., Kaye A., H., Hill, J., S., ‘’ Photodynamic Therapy of Brain Tumors’’, *Journal of Clinical Laser Medicine & Surgery*, 1996, 14 (5), 251-261.

[14] Rosenthal, M., A., et al., ‘’Phase I and pharmacokinetic study of

photodynamic therapy for high-grade gliomas using a novel boronated porphyrin'', *Journal of Clinical Oncology,* 2001, 19 (2), 519-524.

[15] Schweitzer, V., G., ''Photodynamic Therapy for Treatment of Head and Neck Cancer'', *Otolaryngology Head and Neck Surgery,* 1990, 102 (3), 225-232.

[16] Biel, M., A., ''Photodynamic Therapy and the Treatment of Head and Neck Neoplasia'', *The Laryngoscope,* 1998, 108 (9), 1259-1268.

[17] Dougherty, T., J., et al., ''Photoradiation in the Treatment of Recurrent Breast Carcinoma'', *Journal of the National Cancer Institute,* 1979, 62 (2), 231-237.

[18] Mang, T., S., et al., ''A phase II/III clinical study of tin ethyl etiopurpurin (purlytin)-induced photodynamic therapy for the treatment of recurrent cutaneous metastatic breast cancer'', *The Cancer Journal from Scientific American*, 1998, 4 (6), 378.

[19] Dimofte, A., et al., ''In Vivo Light Dosimetry for Motexalin Lutetium-Mediated PDT of Recurrent Breast Cancer'', *Lasers in Surgery and Medicine,* 2002, 305-312.

[20] Gomer, C., J., et al., ''Hematoporphyrin Derivative Photoradiation Therapy for the Treatment of Intraocular Tumors: Examination of Acute Normal Ocular Tissue Toxicity'', *Cancer Research*, 1983, 43 (2), 721-727.

[21] Favilla, I., et al., ''Photodynamic therapy: a 5-year study of its effectiveness in the treatment of posterior uveal melanoma, and evaluation of

haematoporphyrin uptake and photocytotoxicity of melanoma cells in tissue culture'', *Melanoma Research*, 1995, 5 (5), 355-364.

[22] Landau, I., M., E., Steeni B., Seregard, S., ''Photodynamic therapy for circumscribed choroidal haemangioma'', *Acta Ophthalmologica Scandinavica*, 2002, 80 (5), 531-536.

[23] Bown, S., G., et al., ''Photodynamic therapy for cancer of the pancreas'', *Gut*, 2002, 50 (4), 549-557.

[24] Hornung, R., ''Photomedical Approaches for the Diagnosis and Treatment of Gynecologic Cancers'', *Current Drug Targets-Immune, Endocrine & Metabolic Disorders*, 2001, 1 (2), 165-177.

[25] Fehr, M., K., et al., ''Photodynamic Therapy of Vulvar Intraepithelial Neoplasia III Using Topically Applied 5-Aminolevulinic Acid'', *Gynecologic Oncology*, 2001, 80 (1), 62-66.

[26] Hasan, T., et al., ''Photodynamic Therapy of Cancer'', *Cancer Medicine*, 2003, 7, 48-537.

[27] Stolik, S., Delgado, J., A., Perez, A., Anasagasti, L., ''Measurement of the penetration depths of red and near infrared light in human "ex vivo" tissues'', *Journal of Photochemistry and Photobiology A: Chemistry*, 2000, 57, 90–93.

[28] Sullivan, R., Graham, C., H., ''Hypoxia-driven selection of the metastatic phenotype'', *Cancer and Metastasis Reviews*, 2007, 26 (2), 319-331.

[29] Castano, A., P., Demidova, T., N., Hamblin, M., R., ''Mechanisms in

photodynamic therapy: part one—photosensitizers, photochemistry and cellular localization'', *Photodiagnosis and Photodynamic Therapy*, 2004, 1 (4), 279-293.

[30] Robertson, C., A., Hawkins Evans, D., Abrahamse, H., ''Photodynamic therapy (PDT): A short review on cellular mechanisms and cancer research applications for PDT'', *Journal of Photochemistry and Photobiology B: Biology*, 2009, 96 (1), 1-8.

[31] Agostinis, P., et al., '' Photodynamic therapy of cancer: An update'', *CA: A Cancer Journal for Clinicians*, 2011, 61 (4), 250-281.

[32] Monguzzi, A., Tubino, R., Meinardi, F., ''Upconversion-induced delayed fluorescence in multicomponent organic systems: Role of Dexter energy transfer'', *Physical Review B*, 2008, 77 (15), 155122.

[33] Dai, T. et al., ''Concepts and principles of photodynamic therapy as an alternative antifungal discovery platform'', *Frontiers in Microbiology*, 2012, 3.

[34] Kolemen, S., *''Fluorescence Detection of Biological Thiols and Axially Chiral Bodipy Derivatives & Alternative Methodologies for Singlet Oxygen Generation for Photodynamic Action''*, *Dissertation*, 2014.

[35] Turksoy, Abdurrahman, *''Generation, Storage and Delivery of Singlet Oxygen by a Multifunctional Agent''*, *Thesis*, 2017.

[36] Kamkaew, A., et al., ''BODIPY Dyes in Photodynamic Therapy'', *Chemical Society Reviews*, 2013, 42 (1), 77-88.

[37] Hajri, A., et al., ‘’In Vitro and In Vivo Efficacy of Photofrin® and Pheophorbide a, a Bacteriochlorin, in Photodynamic Therapy of Colonic Cancer Cells’’, *Photochemistry and Photobiology*, 2002, 75 (2), 140–148.

[38] Adrasik, S., J., *‘’Singlet Oxygen Generation Using New Fluorene-Based Photosensitizers Under One- and Two-Photon Excitation’’*, *Dissertation,* 2007.

[39] Parkhots, M., V., Lapina, V., A., Butorina, D., N., Sobchuk, A., N., Lepeshkevich, S., V., Petrov, P., T., Krasnovski, Ibreve, Jr, A., A., Dzhagarov, B., M., ‘’Spectral and Photochemical Characteristics of the Photosensitizers Chlorin and Photolon in the Presence of Melanin’’, *Optics & Spectroscopy*, 2005, 98 (3), 374-382.

[40] Datta, S., N., Loh, C., S., MacRobert, A., J., Whatley, S., D., Matthews, P., N., ‘’Quantitative studies of the kinetics of 5-aminolaevulinic acid-induced fluorescence in bladder transitional cell carcinoma’’, *Br J Cancer*, 1998, 78 (8), 1113-8.

[41] Brown, S., B., ‘’The role of light in the treatment of non-melanoma skin cancer using methyl aminolevulinate’’, *Journal of Dermatological Treatment*, 2003, 14, 11.

[42] Zhao, J. Z.; Wu, W. H.; Sun, J. F.; Guo, S. ‘’Triplet photosensitizers: from molecular design to applications’’, *Chemical Society Reviews*, 2013, 42, 5323-5351.

[43] Kobayashi, H., Ogawa, M., Alford, R., Choyke, P., L., and Urano, Y.,

‘‘New Strategies for Fluorescent Probe Design in Medical Diagnostic Imaging’’, *Chemical Reviews*, 2010, 110 (5), 2620-2640.

[44] Kolemen, S., Işık, M. Kim, G., M., Kim, D., Geng, H., Buyuktemiz, M., Karatas, T., X., F., Zhang, Dede, Y., Yoon, Akkaya, E. U. ‘’Intracellular Modulation of Excited-State Dynamics in a Chromophore Dyad: Differential Enhancement of Photocytotoxicity Targeting Cancer Cells’’, *Angewandte Chemie International Edition*, 2015, 127 (18), 5430-5434.

[45] Juzeniene, A., Nielsen, K., P., Moan, J., ‘’Biophysical aspects of photodynamic therapy’’, *Journal of Environmental Pathology, Toxicology and Oncology*. 2006, 25, 7-28.

[46] Wilson, B., C., Jeeves, W., P., Lowe, D., M., ‘’In Vivo and Post Mortem Measurements of the Attenuation Spectra of Light in Mammalian Tissues’’, *Photochemistry and Photobiology*, 1985, 42 (2), 153-162.

[47] Schmidt, M., H., et al., ‘’Light-Emitting Diodes as a Light Source for Intraoperative Photodynamic Therapy’’, *Neurosurgery*, 1996, 38 (3), 552-557.

[48] Foote, C., S., ‘’Mechanism of Photosensitized Oxidation’’, *Science*, 1968, 58 (1), 11-18.

[49] Xiao, Z., Halls, S., Dickey, D., Tulip, J., and Moore, R., B., ‘’Fractionated versus Standard Continuous Light Delivery in Interstitial Photodynamic Therapy of Dunning Prostate Carcinomas’’, *Clinical Cancer Research*, 2007, 13 (24), 7496-7505.

[50] Yang, L., Wei, Y., Xing, D., Chen, Q., ‘’Increasing the efficiency of photodynamic therapy by improved light delivery and oxygen supply using an anticoagulant in a solid tumor model’’, *Lasers in Surgery and Medicine*, 2010, 42 (7), 671-679.

[51] Kolemen, S., Ozdemir, T., Lee, D., Mi Kim, G., Karatas, T., Yoon, J., Akkaya, E.U., ‘’ Remote-Controlled Release of Singlet Oxygen by the Plasmonic Heating of Endoperoxide-Modified Gold Nanorods: Towards a Paradigm Change in Photodynamic Therapy’’, *Angewandte Chemie International Edition*, 2016, 128 (11), 3670-3674.

[52] Redmond, R. W., Kochevar, I. E., “Spatially Resolved Cellular Responses to Singlet Oxygen”, *Photochemistry and Photobiology*, 2006, 82 (5), 1178-1186.

[53] Baader, W. J., Stevani, C. V., Bechara, E. J. H., “Photochemistry Without Light’’, *Journal of the Brazilian Chemical Society*, 2015, Vol. 26 (12), 2430-2447.

[54] Moan, J., Berg, K., ‘’The Photodegradation of Porphyrins in Cells Can Be Used to Estimate the Lifetime of Singlet Oxygen’’, *Photochemistry and Photobiology*, 1991, 53 (4), 549-553.

[55] Foote, C., S., Clennan, E., L., “Properties and Reactions of Singlet Dioxygen”, *Active Oxygen in Chemistry*, 1995, 105-140.

[56] DeRosa, M. C., Crutchley, R. J., “Photosensitized Singlet Oxygen and Its Applications”, *Coordination Chemistry Reviews* 233 - 234, 2002, 351-371.

[57] Devasagayam, T., P., Kamat, J., P., ‘’Biological significance of singlet oxygen’’, *Indian Journal of Experimental Biology*, 2002, 40 (6), 680-692.

[58] Halliwell, B., John, M., C., *Free Radical in Biology and Medicine,* (1982), Second Edition, Clarwndon Press. OxFord.

[59] Kanofsky, J., R., ‘’Singlet Oxygen Production by Biological Systems’’, *Chemico-Biological Interactions*, 1989, 70(1-2), 1-28.

[60] Moureu, C., Marshall, P., ‘’Un Peroxyde Organique Dissociable: Le Peroxyde De Rubrene’’, *Comptes Rendus Chimie,* 1926, 182, 1584-1587.

[61] Fritzsche, M., ‘’Note Sur Les Carbures D'Hydrogene Solides, Tires Du Goudron De Houille’’, *Comptes Rendus Chimie*, 1867, 64, 1035-1037.

[62] Günther, Schenck, O., Ziegler, K., ‘’Die Synthese des Ascaridols’’, *Die Naturwissenschaften,* 1944, 32 (14), 157.

[63] Foote C. S., Wexler S., ‘’Olefin Oxidations with Excited Singlet Molecular Oxygen’’, *Journal of American Chemical Society*, 1964, 86 (18), 3879-3880.

[64] Evans, D. F., ‘’Oxidation by photochemically produced singlet states of oxygen’’, *Journal of the Chemical Society D: Chemical Communications,* 1969, (7), 367-368.

[65] Hideg É., Kálai, T., Kós, P., B., Asada, K., Hideg K., ‘’Singlet Oxygen in Plants-Its Significance and Possible Detection with Double (Fluorescent and Spin) Indicator Reagents’’, *Photochemistry Photobiology*, 2006, 82 (5), 1211-1218.

[66] Scurlock, R. D., Wang, B., Ogilby, P. R., Sheats, J. R.; Clough, R. L., ‘’Singlet Oxygen as a Reactive Intermediate in the Photodegradation of an Electroluminescent Polymer’’, *Journal of American Chemical Society*, 1995, 117 (41), 10194-10202.

[67] Tørring, T., Helmig, S., Ogilby, P., R., Gothelf, K., V., “Singlet Oxygen in DNA Nanotechnology”, *Accounts of Chemical Research*, 2014, 47, 1799 – 1806.

[68] Ozlem, S.; Akkaya. E. U., ‘’Thinking outside the silicon box: molecular and logic as an additional layer of selectivity in singlet oxygen generation for photodynamic therapy.’’ *Journal of the American Chemical Society*, 2009, 131 (1), 48–49.

[69] Shao, A., et al., ‘’Far-Red and Near-IR AIE-Active Fluorescent Organic Nanoprobes with Enhanced Tumor-Targeting Efficacy: Shape-Specific Effects’’, *Angewandte Chemie International Edition*, 2015, 127 (25), 7383–7388.

[70] Simsek, Turan, I., Pir, Çakmak, F., Yildirim, D., C., Cetin, Atalay, R., Akkaya, E., U., ‘’Near-IR Absorbing BODIPY Derivatives as Glutathione-Activated Photosensitizers for Selective Photodynamic Action’’, *Chemistry of European Journal*, 2014, 20 (49), 16088–16092.

[71] Foote, C., ‘’Mechanism of addition of singlet oxygen to olefins and other substrates.’’ *Pure and Applied Chemistry*, 1971, 27(4), 635-646.

[72] Bobrowski, M., Liwo, A., Ołdziej, S., Jeziorek, D. and Ossowski, T., ‘’CAS MCSCF/CAS MCQDPT2 Study of the Mechanism of Singlet Oxygen Addition

to 1,3-Butadiene and Benzene'', *Journal of the American Chemical Society*, 2000, 122 (34), 8112-8119.

[73] Aubry, J. M., Pierlot, C., Rigaudy, J., Schimdt, R., ''Reversible binding of oxygen to aromatic compounds.'' *Accounts of Chemical Research*, 2003, 36 (9), 668-675.

[74] Atkins, P. and de Paula, J., ''Physical Chemistry'', 2006, 74 (16), 706.

[75] Van den Heuvel, C. J. M., Verhoeven, J. W., de Boer, Th. J., ''A frontier orbital description of the reaction of singlet oxygen with simple aromatic systems'', *Recueil des Travaux Chimiques des Pays-Bas*, 1980, 99 (9), 280-284.

[76] Aubry, J. M., Mandard-Cazin, B., Rougee, M. and Bensasson R. V., '' Kinetic Studies of Singlet Oxygen [4 + 2]-Cycloadditions with Cyclic 1,3-Dienes in 28 Solvents'', *Journal of the American Chemical Society*, 1995, 117 (36), 9159-9164.

[77] Turro, N. J., Chow M. F. and Rigaudry J., ''Mechanism of thermolysis of endoperoxides of aromatic compounds. Activation parameters, magnetic field, and magnetic isotope effects'', *Journal of the American Chemical Society*, 1981, 103 (24), 7218-7224.

[78] Slavětínská, L., Mosinger, J., Kubát, P., ''Supramolecular carriers of singlet oxygen: Photosensitized formation and thermal decomposition of endoperoxides in the presence of cyclodextrins'', *Journal of Photochemistry and Photobiology A: Chemistry*, 2008, 195 (1), 1–9.

[79] Ben-Shabat, S., Itagaki, Y., Jockusch, S., Sparrow, J. R., Turro, N. J., Nakanishi, K., ‘’ Formation of a Nonaoxirane from A2E, a Lipofuscin Fluorophore related to Macular Degeneration, and Evidence of Singlet Oxygen Involvement’’, *Angewandte Chemie International Edition,* 2002, 41 (59), 814-817.

[80] Saito, I., Matsuura, T., Inoue, K., ‘’Formation of Superoxide Ion from Singlet Oxygen on the Use of a Water-Soluble Singlet Oxygen Source’’, *Journal of the American Chemical Society*, 1981, 103, 188-190.

[81] Nieuwint, A. W., Aubry J. M., Arwert, F., Kortbeek, H., Herzberg, S., Joenje, H., ‘’Inability of chemically generated singlet oxygen to break the DNA backbone’’, *Free Radical Research Communications*, 1985, 1(1), 1-9.

[82] Matsumoto, M., Yamada, M. and Watanabe, N., ‘’Reversible 1,4-cycloaddition of singlet oxygen to N-substituted 2-pyridones: 1,4-endoperoxide as a versatile chemical source of singlet oxygen’’, *Chemical Communications*, 2005, (4), 483-485.

[83] Simsek Turan, I., Yildiz, D., Turksoy, A., Gunaydin, G., Akkaya, E., U., ‘’A Bifunctional Photosensitizer for Enhanced Fractional Photodynamic Therapy: Singlet Oxygen Generation in the Presence and Absence of Light’’, *Angewandte Chemie International Edition*, 2016, 55(8), 2875-2878.

[84] Chantong, C., Carney, D., Luo, L., et al. ‘’A porphyrin molecule that generates, traps, stores, and releases singlet oxygen’’, *Journal of Photochemistry*

and Photobiology A-Chemistry, 2013, 260, 9-13.

[85] Benz, S., Notzli, S., Siegel, J., Eberli, D., Jessen, H., ‘’Controlled Oxygen Release from Pyridone Endoperoxides Promotes Cell Survival under Anoxic Conditions’’, *Journal of Medicinal Chemistry*, 2013, 56(24), 10171-10182.

[86] Lin, H., Shen, Y., Chen, D., Lin, L., Wilson, B., C., Li, B., Xie, S., ‘’Feasibility Study on Quantitative Measurements of Singlet Oxygen Generation Using Singlet Oxygen Sensor Green’’, *Journal of Fluorescence*, 2013, 23 (1), 41–47.

[87] Yang, L., Finney, N., S., ‘’A mechanistically-distinct approach to fluorescence visualization of singlet oxygen’’, *Chemical Communications*, 2017, 53, 11449-11452.

[88] Gollmer, A., Arnbjerg, J., Blaikie, F., H., Pedersen, W., B., Breitenbach, T., Daasbjerg, K., Glasius, M., and Ogilby, P., R., ‘’Singlet Oxygen Sensor Green: Photochemical Behavior in Solution and in a Mammalian Cell’’, *Photochemistry and Photobiology*, 2011, 87, 671–679.

[89] Gossweiler G., R., et al., ‘’Mechanochemical Activation of Covalent Bonds in Polymers with Full and Repeatable Macroscopic Shape Recovery ‘’, *ACS Macro Letters*, 2014, 3, 216−219.

CHAPTER VI

Appendices

^{1}H, ^{13}C NMR Spectra and

Thermogravimetric Analysis

Appendix A: ^{1}H and ^{13}C NMR Spectra

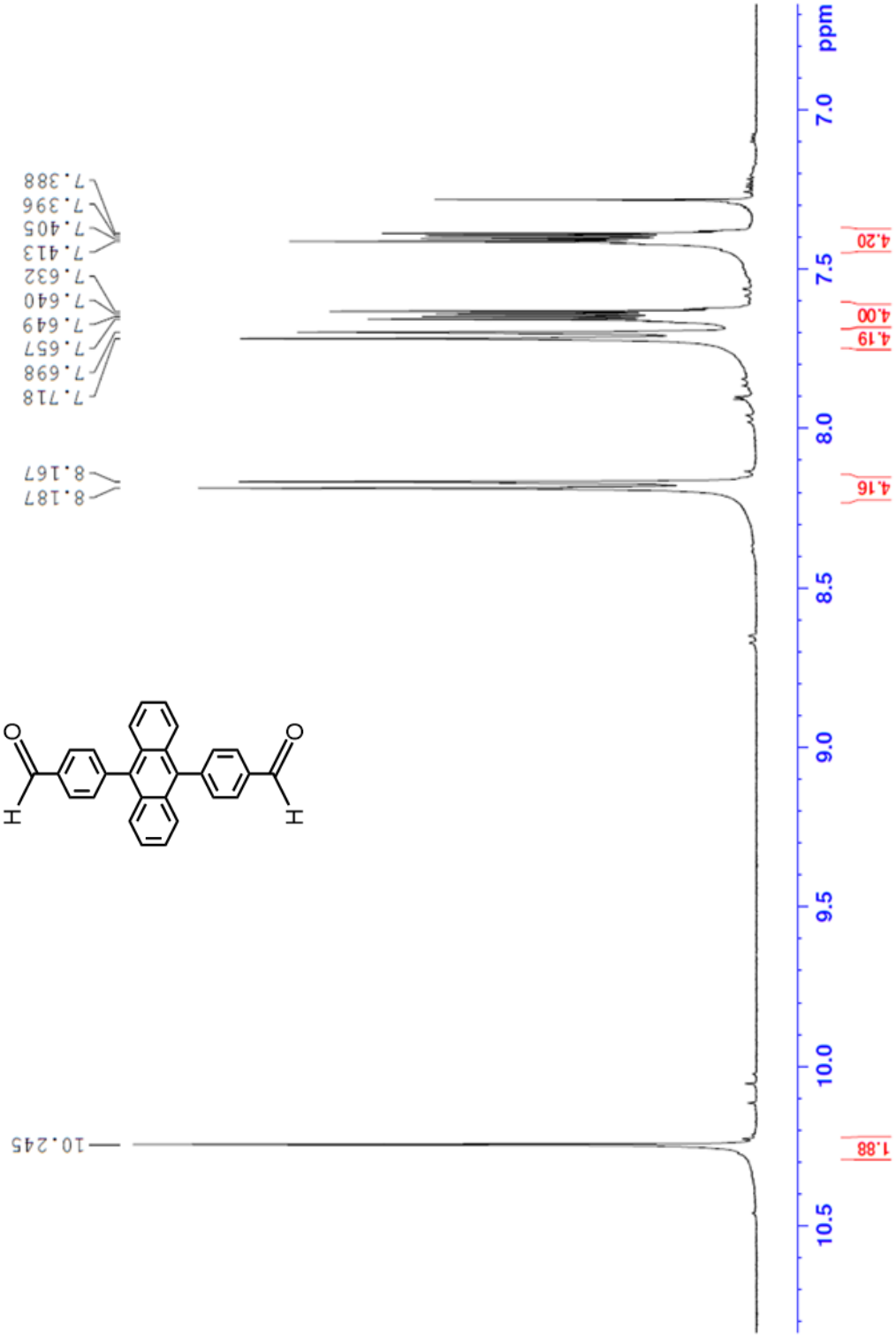

Figure 44: ^{1}H NMR Spectrum of Compound **20** in $CDCl_3$

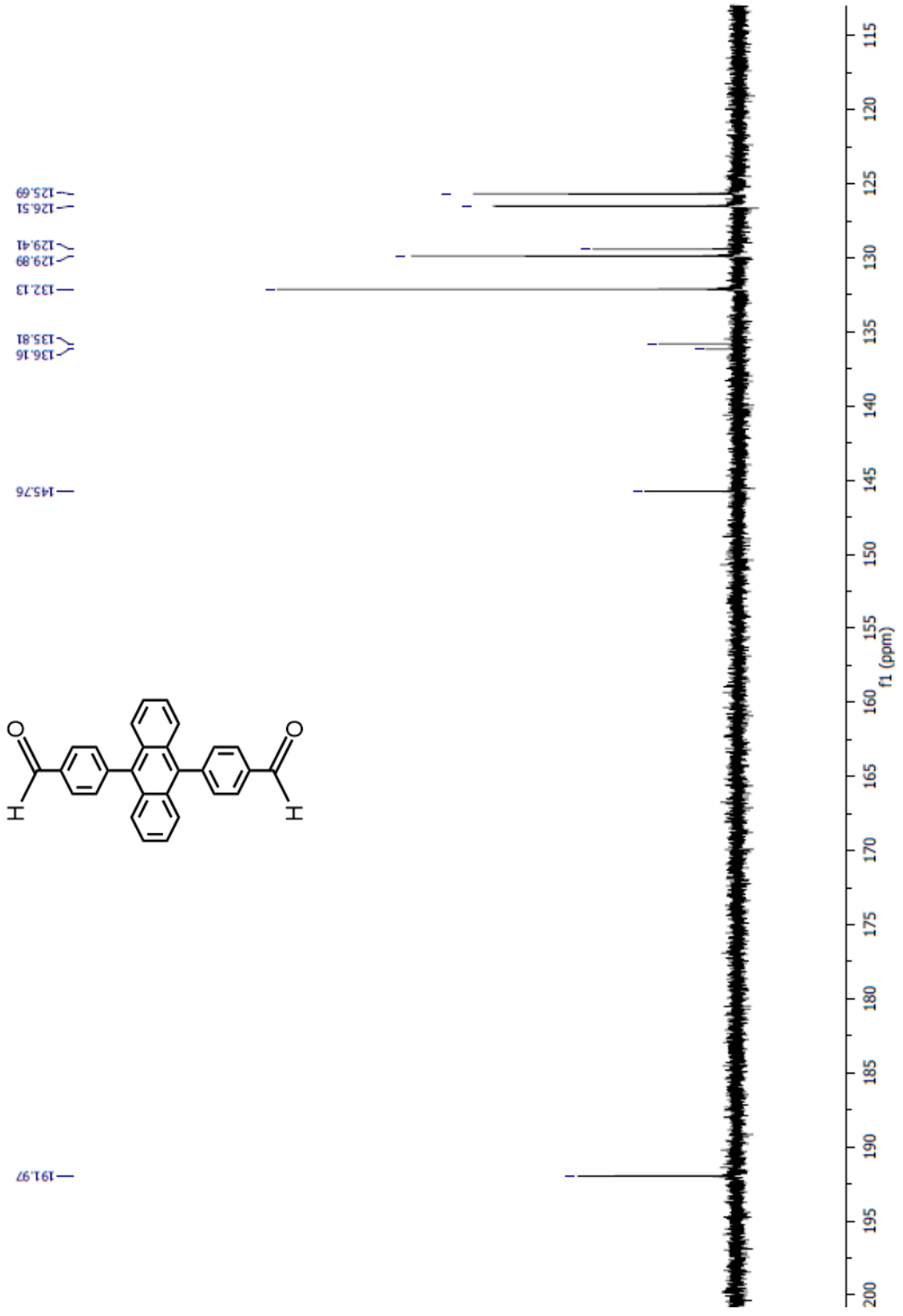

Figure 45: ^{13}C NMR Spectrum of Compound **20** in $CDCl_3$

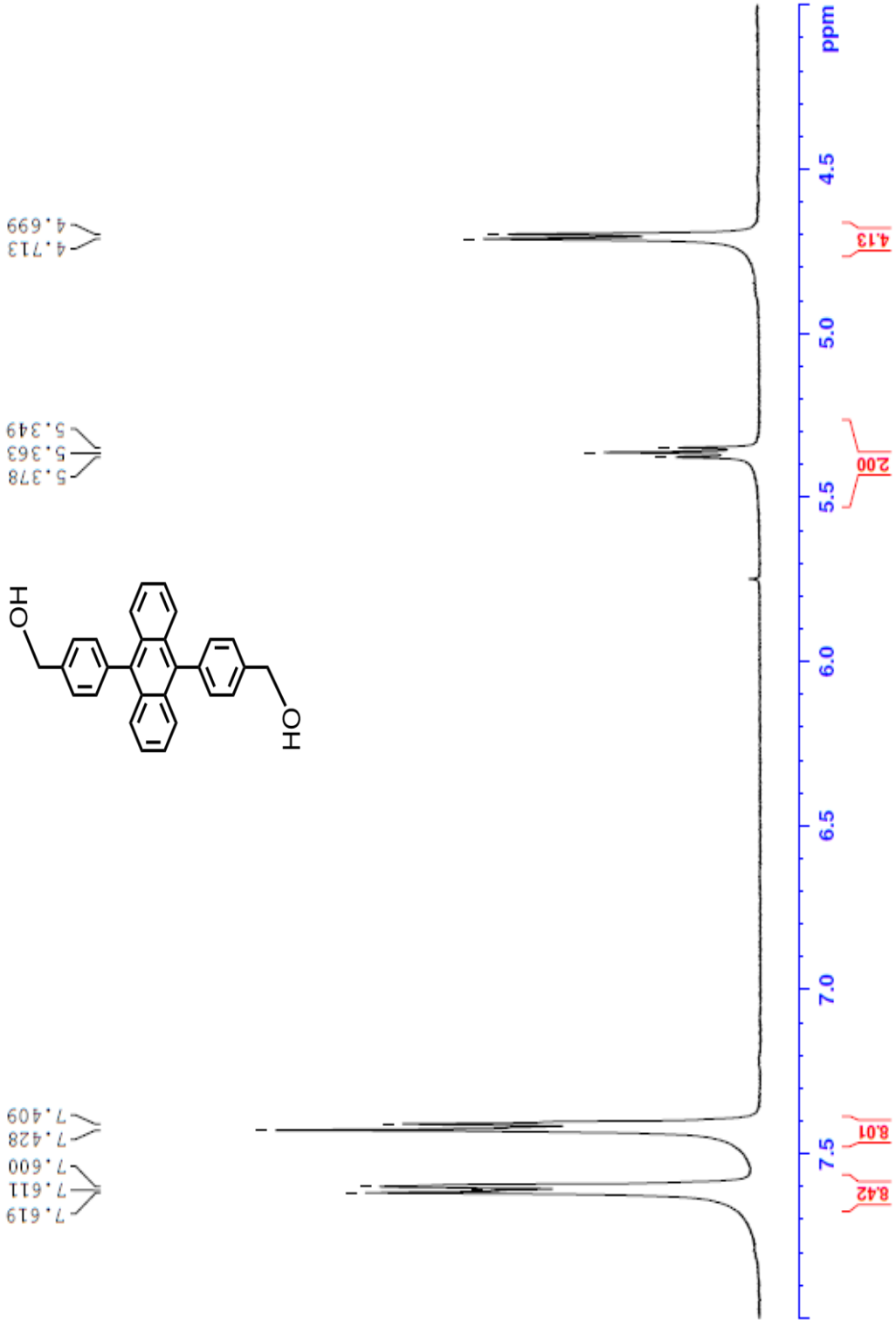

Figure 46: ^{1}H NMR Spectrum of Compound **21** in DMSO-d_6

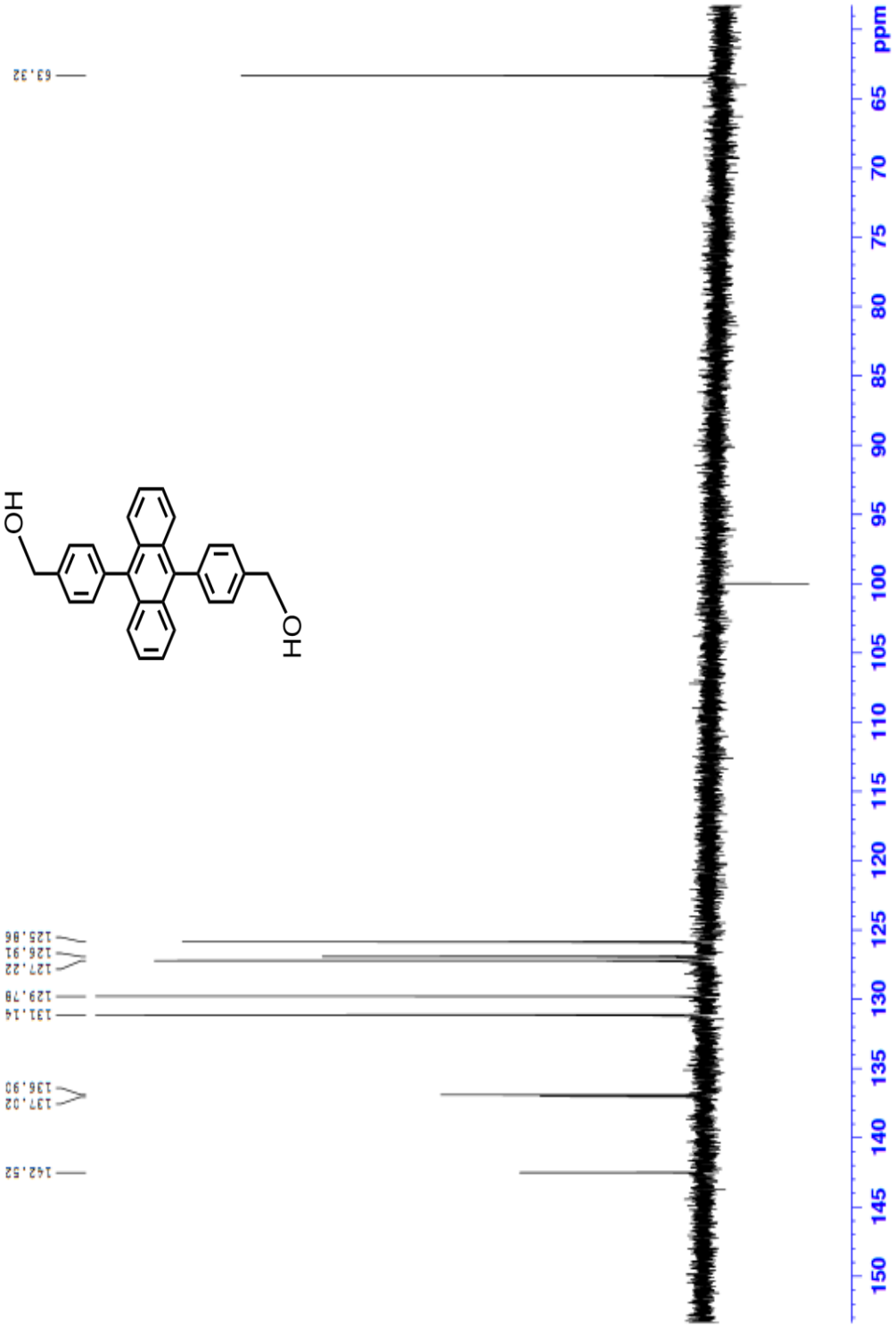

Figure 47: ^{13}C NMR Spectrum of Compound **21** in DMSO-d_6

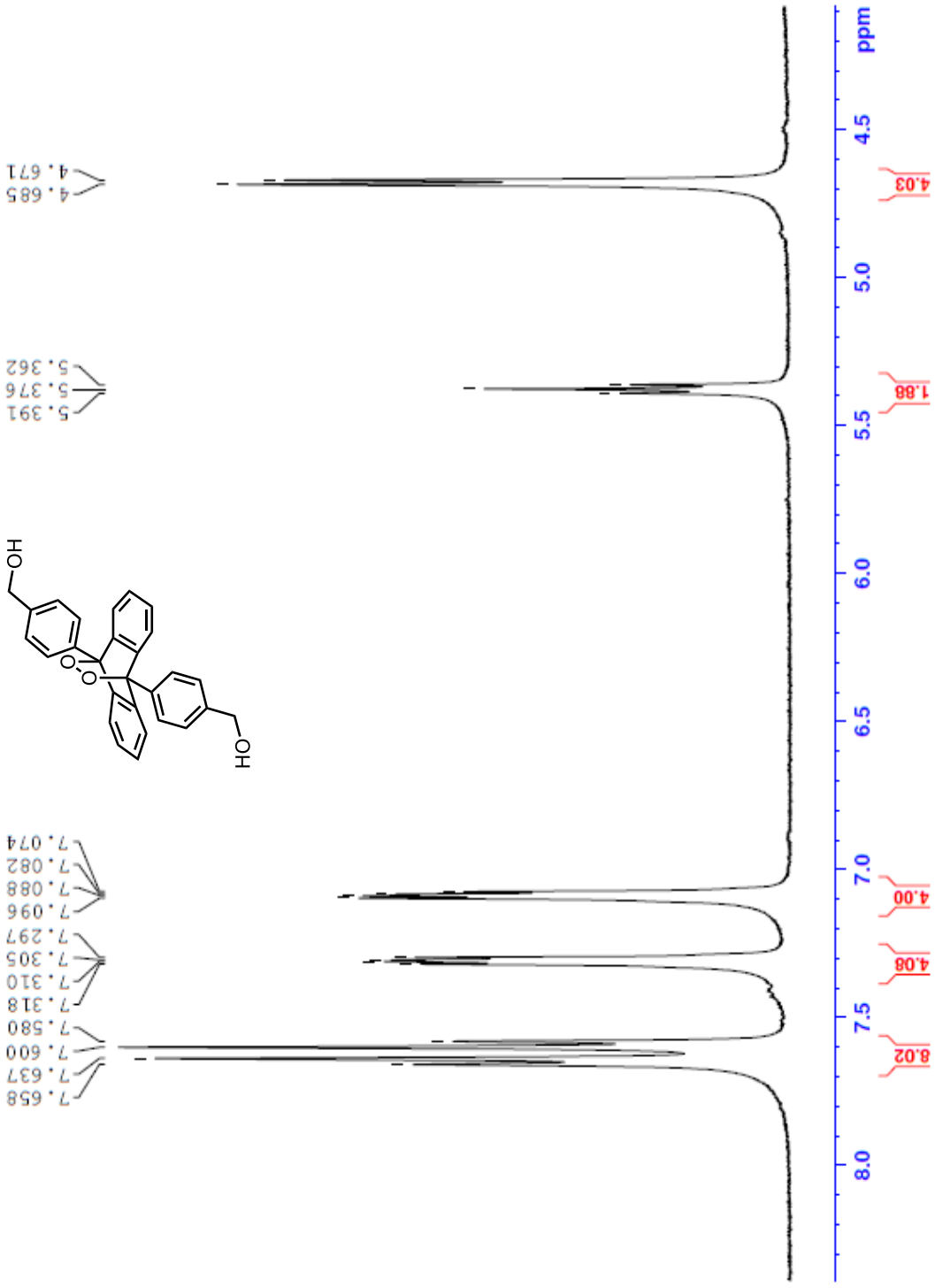

Figure 48: ^{1}H NMR Spectrum of Compound **22** in DMSO-d_6

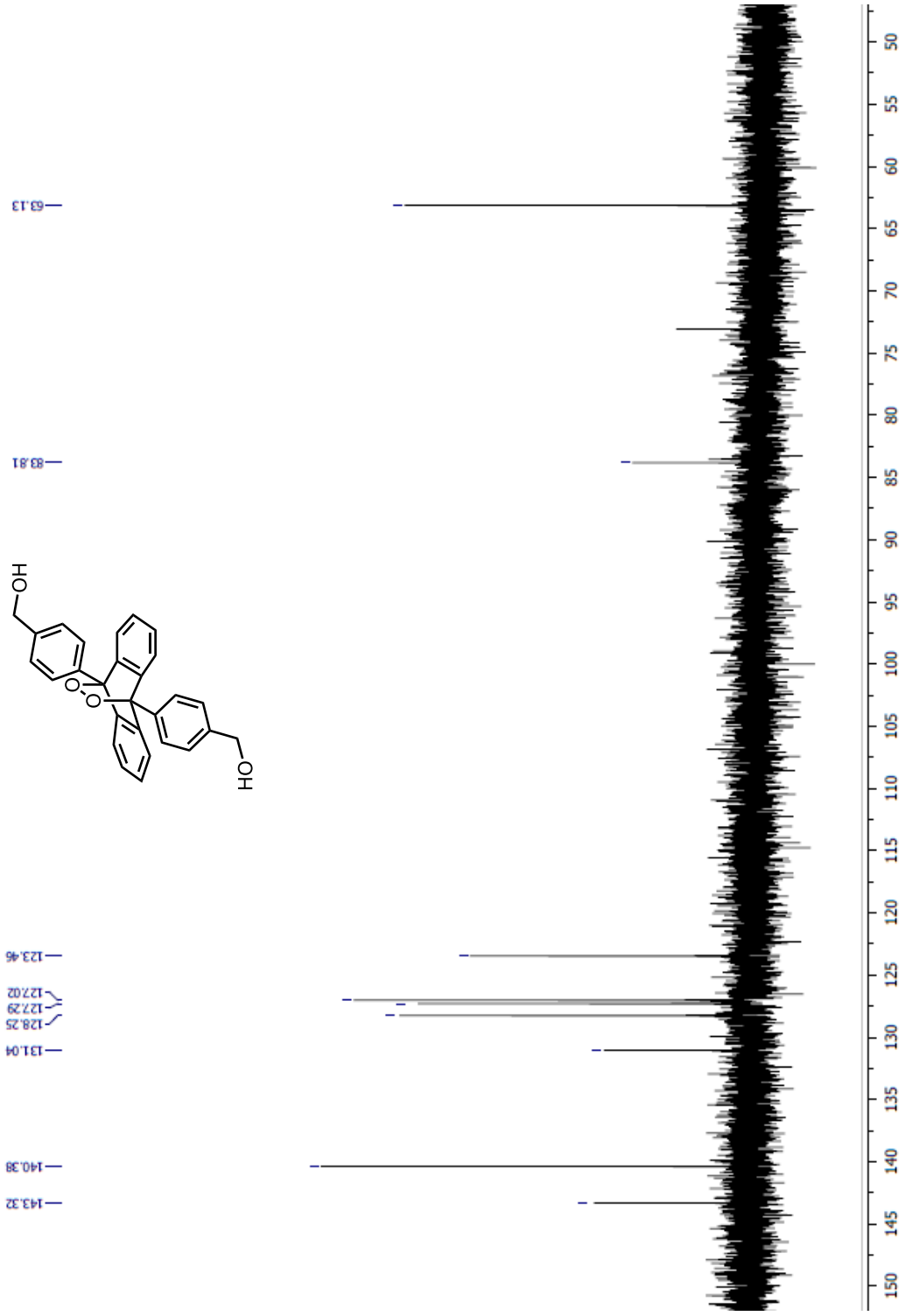

Figure 49: ^{13}C NMR Spectrum of Compound **22** in DMSO-d_6

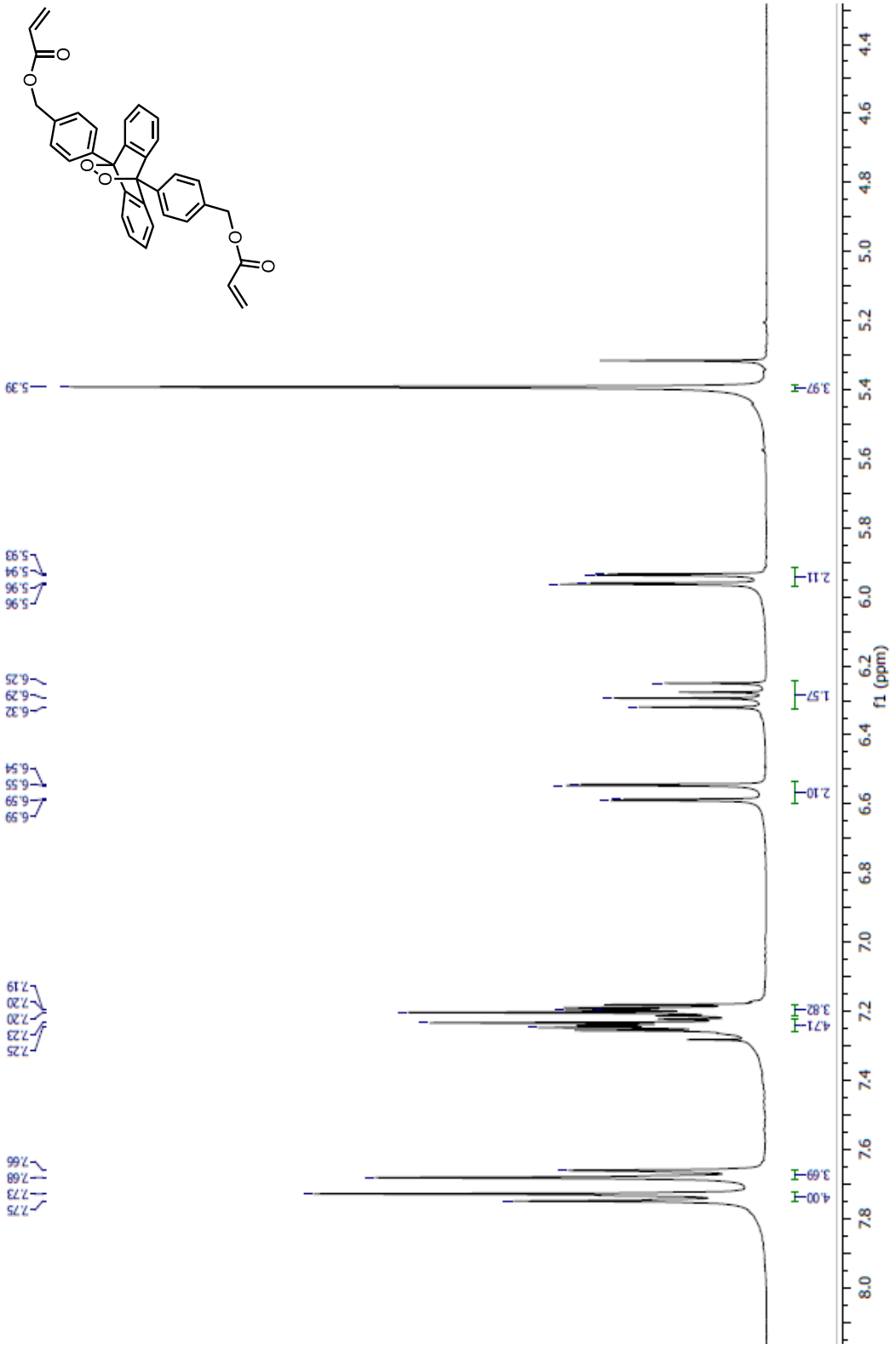

Figure 50: ^{1}H NMR Spectrum of Compound **23** (crosslinker) in $CDCl_3$

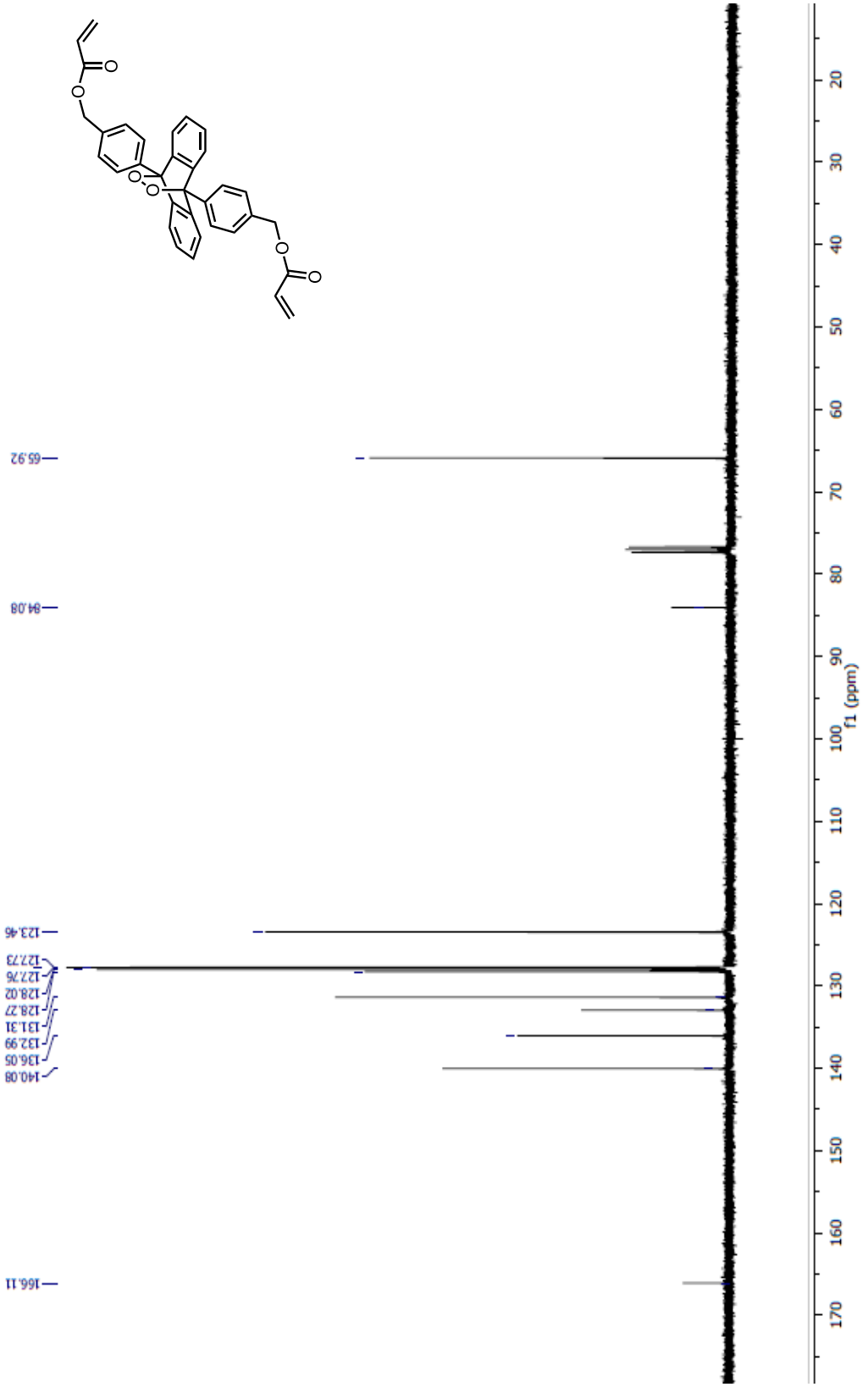

Figure 51: ^{13}C NMR Spectrum of Compound **23** (crosslinker) in $CDCl_3$

Appendix B: Thermogravimetric Analysis

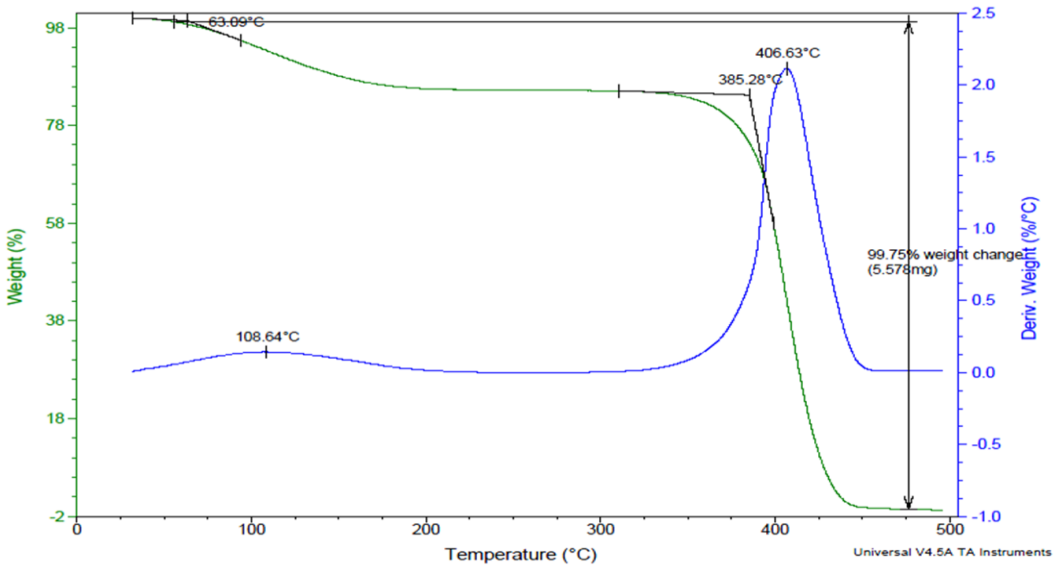

Figure 52: TGA Thermogram for PMA-EPO **(24)** with 10^0C/min heating rate under nitrogen atmosphere.